A Review on Methods for State of Health Forecasting of Lithium-Ion Batteries applicable in Real-World Operational Conditions

Friedrich von Bülow[a*] and Tobias Meisen[b]

[a] *Volkswagen AG, Berliner Ring 2, 38436 Wolfsburg, Germany*

[b] *Institute of Technologies and Management of the Digital Transformation, University of Wuppertal, Rainer-Gruenter-Str. 21, 42119, Wuppertal, Germany*

*Corresponding author: Friedrich von Bülow, E-mail address: friedrich.von.buelow@volkswagen.de, Postal address: Volkswagen AG, Berliner Ring 2, 38436 Wolfsburg, Germany

Abstract

The ageing of Lithium-ion batteries can be described as change of state of health (ΔSOH). It depends on the battery's operation during charging, discharging, and rest phases. Mapping the operation conditions during these phases for long time windows to a ΔSOH enables forecasting the battery's SOH. With SOH forecasting fleet managers of battery electric vehicle (BEV) fleets can plan vehicle replacement and optimize the fleet's operational strategy. Inspired by the applicability from a user's perspective of fleet managers and battery designers, this work motivates and defines key criteria for SOH forecasting models. The key criteria concern the encoding of information in the model inputs, model transferability to other batteries, and the applicability to 2nd life battery applications. Based on these key criteria we review SOH forecasting models. Currently, only few models satisfy the majority of the defined key criteria, while three others only fail at two key criteria. The majority (71 %) of the methods use machine learning models which can be seen as current research trend due to the complex dependence of battery operational data and battery ageing. We show limitations of the applicability and comparability of existing models due to different data sets, different metrics, different output values, and different forecast horizons. Furthermore, code and data are only rarely shared and publicly available.

Keywords: Lithium-ion battery; battery electric vehicles; state of health; battery ageing; forecasting; machine learning

1 Introduction

With worldwide rising registrations of new battery electric vehicles (BEV) the battery's state of health (SOH) becomes a priority of customers, researchers, and industrials [1,2]. The SOH compares the current state of the battery to the state of a new battery at its beginning of life (BOL) and depends on the usage and environmental conditions of the battery [3–5]. With increasing battery ageing the battery's SOH and the range of BEVs decrease. But also for other battery applications like grid energy storage und electric trains the SOH is relevant [6,7].

In the literature, we observe two methodological principles: SOH estimation and SOH forecasting. First, SOH estimation is the determination of the $SOH(t)$ at a certain point in time t. SOH estimation for future SOH is often called SOH prediction in the literature when applicability in the future is doubtful. Second, battery ageing is a state change of the SOH from a current $SOH(t_1)$ to a future $SOH(t_2)$ due to ageing causes. SOH forecasting is predicting this state change (ΔSOH) or the future $SOH(t_2)$ given information on the battery operational load during the period of time $\Delta t = t_2 - t_1$ until the future point in time t_2. Thus, compared to SOH forecasting, the SOH estimation does not model a change in state, but only a determination of state.

Within many surveys, different methods for SOH estimation of batteries are examined and compared [8–11]. The same applies for predicting of the remaining useful life (RUL) which provides similar information like the SOH [12,13]. Some surveys also address both [14–16]. Thereby, the applicability of the reviewed methods is limited for SOH forecasting because they lack input information on the future battery operational load. This means the methods assume the same load from the past also in the future. However, as Lucu et al. [17] note, batteries in real-world operation, e.g. in automotive applications, exhibit varying loads during the battery's lifetime. Therefore, information about the future operating load of the battery is essential for a SOH forecast.

A study by Badey et al. [18] with similar subject matter is ten years old: In it methods for SOH forecasting, such as physically based models (equivalent circuit models (ECM) and empirical models), mathematical models (artificial neural network (ANN)), and fatigue models (Wöhler and Weighted-Ah method) are investigated. However, this study does not define key criteria for a structured comparison of the different methods. A review by Collath et al. [19] published 2022 is examining methods for aging aware operation of battery energy storage systems (BESS), e.g. for peak shaving or Vehicle-To-Grid (V2G) applications. Their focus is on scheduling of stationary batteries but not on battery operation in automotive applications.

A model for SOH forecasting becomes necessary in several application areas. For example, cloud-based fleet services depend on suitable SOH forecasting models. Assuming a certain usage scenario of a BEV fleet, the fleet manager can forecast the battery SOH of the fleet's vehicles and knows, when a vehicle replacement due to battery deterioration will be required. Furthermore, battery designers can conduct virtual battery ageing experiments by adapting the usage scenario data. As an example, the maximum discharge current can be limited above a certain temperature threshold. After adapting the usage scenario data, the model will output its effect on the SOH. This enables a prescriptive analysis and recommendations for an operational strategy for BEV fleets including fleet charging management.

Another model application is related to 2nd life screening: Old cells with similar SOH shall be grouped together to be assembled as new battery packs for 2nd life applications [20,21]. Determining the current SOH is the task of SOH estimation. However, it will be beneficial if the future SOH of the cells stays similar. This can be ensured by SOH forecasting, especially by probabilistic SOH forecasting.

Furthermore, SOH forecasting models can be applied for matching batteries at the end of their 1st life. Potential 2nd life applications like BESS for grid energy are specified by operational conditions and an EOL criterion. Given these operational conditions of the 2nd life, users could back-calculate a minimum required SOH after 1st life that ensures meeting the 2nd life EOL criterion. The same way users can adapt the operational conditions in 1st life to simulate possible scenarios to transition to 2nd life. Such a model can also be interesting for insurances to cover battery manufacturers warranties [22].

SOH forecasting based on real-world data until now has only rarely been conducted on a large scale because of a lack of publicly available data. Only now with the transition to BEVs more data becomes available. Especially intensive usages of BEVs in fleets for Mobility-as-a-Service (MaaS) are interesting for data collection. However, the use case of MaaS came up first 2017 [23]. Only a year later MOIA started which is the first ride pooling MaaS in Germany [24]. Because of these changes now SOH forecasting becomes more feasible and relevant.

This paper contributes first a) the definition of different SOHs on cell and pack level, b) the comparison of SOH estimation and forecasting, and the comparison of c) SOH and RUL. Second, key criteria are defined for SOH forecasting models motivated by the real-world model application of BEV fleet manager and battery designers. Third, differences of battery operation in laboratory and real-world vehicle operation are summarized. Fourth, a literature survey for SOH forecasting models is conducted based on the previously defined key criteria. Fifth, limitations of applicability and comparability of existing models are discussed.

The remainder of this paper is structured as follows: In Section 2, the object of investigation is specified: SOH and RUL are defined as well as SOH estimation and forecasting get differentiated. Further, this survey and the key criteria are motivated in more detail. In Section 3, we outline how we determined the database for the survey and how we conducted the subsequent screening and analysis. In Section 4, SOH forecasting methods are structured and presented. Section 5 concludes our work.

2 Object of Investigation

2.1 State of Health

The SOH compares the current state of the battery to the state of a new battery at its BOL [3–5]. The SOH can be defined differently depending on the view point, e.g. of a manufacturer and battery user [5]. Any state variable that changes with ageing may be suitable for the definition of the SOH, like the number of charging/discharging cycles [10], the voltage change caused by the load of a power or current profile [25], AC impedance, self-discharge rate, and power density [3,26,27]. These can be used individually or jointly [27], e.g. as a vector, arithmetic mean, or geometric mean. Commonly, the SOH is described by the internal resistance R or the remaining capacity C [28,29]. The resistance-based SOH (SOH_{R}) is the current internal ohmic resistance $R(t)$ relative to the internal ohmic resistance of a new battery R_{nom} [30–32]:[1]

$$SOH_{\mathrm{R}}(t) = \frac{R(t)}{R_{\mathrm{nom}}}. \tag{1}$$

Analogous, the capacity-based SOH (SOH_{C}) denotes the remaining capacity $C(t)$ relative to the nominal capacity C_{nom} which is specified by the battery manufacturer for a certain battery type [5,14,31–33]:[2]

$$SOH(t) = SOH_{\mathrm{C}}(t) = \frac{C(t)}{C_{\mathrm{nom}}}. \tag{2}$$

Usually, C_{nom} is similar to the initial capacity $C(t_0)$ at the BOL of a new battery, i.e. after production, but due to deviations in the manufacturing process there may be differences [14]. Measuring the capacity requires standard operational conditions regarding the temperature and charge-discharge profile [34]. In the following, we focus on the SOH_{C}, for simplicity referred to as SOH because it reflects the energy capability and the range of BEVs. The SOH_{R} would be interesting for hybrid electric vehicles (HEVs) and electric trains, i.e. battery electric multiple units (BEMUs), because it reflects the power capability [6,35,36].

[1] Other definitions of SOH_{R} are presented in the Appendix in Eqs. (33) - (35).
[2] Another definition of SOH_{C} is presented in the Appendix in Eq. (14).

Most literature focuses on the SOH of battery cells. However, in most applications including BEVs, not single battery cells, but battery systems are used. Synonymously to the term battery system sometimes the term battery pack is used [37–40]. A battery pack is an energy storage device composed of one or several electrically connected cells or modules. A battery module is a group of battery cells in series (s) and/or parallel (p) connection [41,42] as depicted in Figure 1 a) and b). Usually, series and parallel circuits are combined: A parallel connection consisting of cells in series connection is called parallel-series (ps) connection as in Figure 1 c). A series connection consisting of cells in parallel connection is called series-parallel (sp) connection as in Figure 1 d). For example, 3s4p abbreviates three cells in series and four in parallel. The amount, connection, and split of the cells into modules and packs depends on the battery application. For further information consider [3,41].

Figure 1: Cells in series (s), parallel (p), parallel-series (ps) and series-parallel (sp) connection.

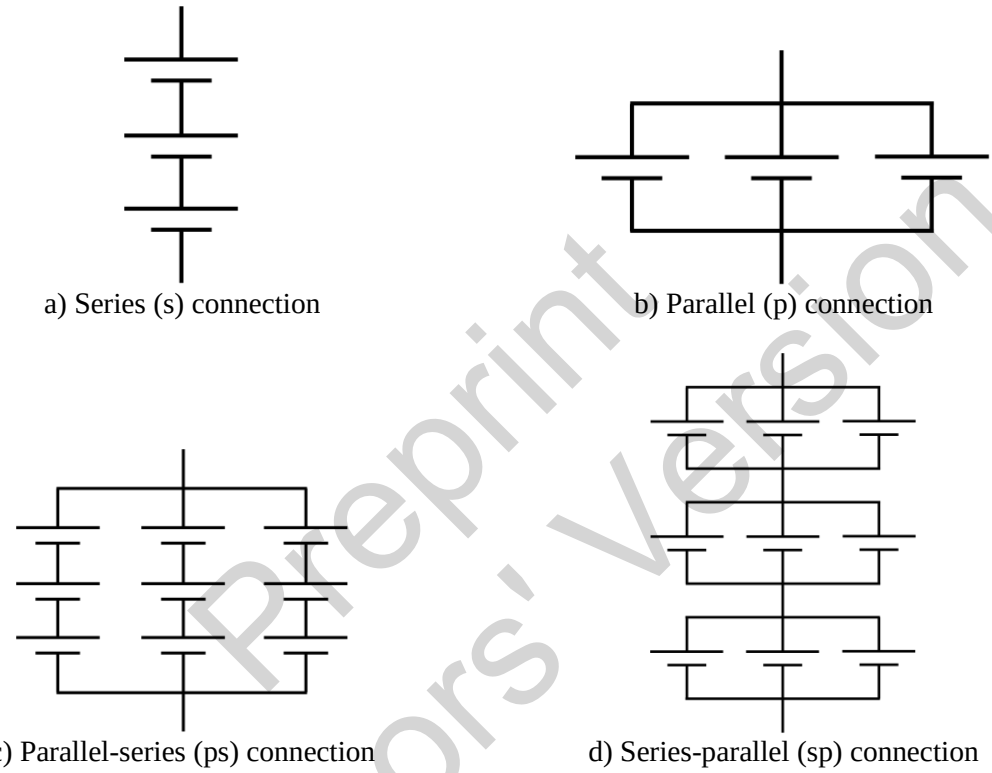

a) Series (s) connection

b) Parallel (p) connection

c) Parallel-series (ps) connection

d) Series-parallel (sp) connection

The battery management system (BMS) protects the battery against failure modes like overcharging, overdischarging, high and low temperatures, as well as short circuiting. It also ensures that the cells in a pack have the same state of charge (SOC), i.e. voltage, which is called cell balancing. Cell balancing maximizes the battery's useable amount of charge because the cell with the lowest voltage determines the end of discharging and the cell with the highest voltage determines the end of charging, both when hitting the respective voltage limits. Active cell balancing is only necessary in series connections, as cells in parallel connection balance each other automatically because of Kirchhoff's voltage law [3].

Warner [3] and Kampker [41] state that the total capacity of a battery pack is limited by the cell with the lowest capacity in the pack. More precisely, this only applies to cells in series connection because the cell with the lowest capacity will reach the voltage limits first [43,44]. The capacity $C_\mathrm{s}(t)$ of n_s cells in series connection is the lowest capacity of the cells in series connection $C_i(t)$ [45,46]:

$$C_\mathrm{s}(t) = \min_i C_i(t) \quad \text{with } i = 1,2,\dots,n_\mathrm{s} \tag{3}$$

assuming that all cells have the same internal resistance $R(t)$.[3]

The capacity $C_{\mathrm{p}}(t)$ of n_{p} cells in parallel connection is the sum of the single cells' capacities $C_j(t)$ following Kirchhoff's current law [46,47]:

$$C_{\mathrm{p}}(t) = \sum_{j=1}^{n_{\mathrm{p}}} C_j(t) \text{ with } j = 1,2,\dots,n_{\mathrm{p}}. \tag{4}$$

With Eqs. (2) and (3) follows, that the SOH of cells in series connection $SOH_{\mathrm{C,s}}(t)$ is the cells' minimal $SOH_{\mathrm{C},i}(t)$ assuming C_{nom} is the same for all cells [45,46,48]:[4]

$$SOH_{\mathrm{C,s}}(t) = \min_i SOH_{\mathrm{C},i}(t) \text{ with } i = 1,2,\dots,n_{\mathrm{s}}. \tag{5}$$

Analogous with Eqs. (2) and (4) follows that the SOH of cells in parallel connection $SOH_{\mathrm{C,p}}(t)$ is the average of all single cells' $SOH_{\mathrm{C},j}(t)$ assuming C_{nom} is the same for all cells [46]:

$$SOH_{\mathrm{C,p}}(t) = \frac{1}{n_{\mathrm{p}}} \sum_{j=1}^{n_{\mathrm{p}}} SOH_{\mathrm{C},j}(t) \text{ with } j = 1,2,\dots,n_{\mathrm{p}}. \tag{6}$$

Thus, a faster degradation of a single cell has a bigger influence on the SOH in a series connection than in a parallel connection. This corresponds with the results of Jeng et al. [44]. Both Eqs. (5) and (6) are derived step by step in the Appendix in Eqs. (15) - (17) and (18) - (19) respectively.[5]

With Eqs. (5) and (6) follows that the $SOH_{\mathrm{C,ps}}(t)$ of cells in parallel-series connection is the sum over all the parallel connections' SOH which each is determined by the minimum SOH of the series connection [46]:

$$SOH_{\mathrm{C,ps}}(t) = \frac{1}{n_{\mathrm{p}}} \sum_{j=1}^{n_{\mathrm{p}}} \min_i SOH_{\mathrm{C},ij}(t) \tag{7}$$

with $i = 1,2,\dots,n_{\mathrm{s}}$, and $j = 1,2,\dots,n_{\mathrm{p}}$, and assuming C_{nom} is the same for all cells.

Analogous with Eqs. (5) and (6) follows that the $SOH_{\mathrm{C,sp}}(t)$ of cells in series-parallel connection is the minimum of all series connections SOH's which each is determined by the minimum SOH of the parallel connection [46]:

$$SOH_{\mathrm{C,sp}}(t) = \frac{1}{n_{\mathrm{p}}} \min_i \sum_{j=1}^{n_{\mathrm{p}}} SOH_{\mathrm{C},ij}(t) \tag{8}$$

with $i = 1,2,\dots,n_{\mathrm{s}}$, and $j = 1,2,\dots,n_{\mathrm{p}}$, and assuming C_{nom} is the same for all cells. Both Eqs. (7) and (8) are derived step by step in the Appendix in Eqs. (20) - (23) and (24) - (27) respectively. Overall, it is desirable to build packs from cells with similar capacity. Also, the SOH of cells in sp connection is greater than or equal to the SOH of cells in ps connection:

[3] Assuming the cells are balanced well and, thus, the open-circuit voltage (OCV) is the same for all cells, still different R_i of cells in series connection lead to different voltage changes with the same current I_{S} on the series connection: $\Delta U_i = I_{\mathrm{S}} \cdot R_i$. So, theoretically R_i also influences which cell hits the voltage limits first. Also, theoretically even for a cell with very high resistance the full capacity could be used with $\lim_{t\to\infty} I(t) \to 0$.

[4] The assumption that C_{nom} is the same for all cells is not made by Juhlin [46] but mathematically necessary. Its fulfillment is given in practice as the same battery cell type is usually built within one battery module or pack.

[5] The SOH_{R} in series and parallel connection is derived in the Appendix in Eqs. (38) - (43) and (44) - (49) respectively.

$$SOH_{\mathrm{C,ps}}(t) \leq SOH_{\mathrm{C,sp}}(t) \tag{9}$$

as derived in the Appendix in Eqs. (28) - (32).

Aging of battery modules and systems is more complex than of a single cell because of the interactions of all cells. It is influenced by inconsistencies of cell characteristics, electrical imbalance, and temperature gradients between cells [15]. For example, Bruen and Marco [49] observe significant differences of cells in parallel regarding their current which results in different temperature distributions and aging of the cells. Jung et al. [50] found that the internal temperature within battery modules is higher than of a single cell because of the transfer of thermal energy to adjacent cells. As with a single cell a higher temperature causes greater capacity fade. If no appropriate thermal management system is cooling the battery modules, a SOH forecasting model would need to consider these changes of the temperature influence on aging.

2.1.1 State of Health Estimation, Prediction and Forecast

In the literature, we observe two methodological principles: SOH estimation and SOH forecasting. First, SOH estimation is the determination of the $SOH(t_\mathrm{e})$ at a certain point in time t_e based on information available at this point in time:

$$SOH(t_\mathrm{e}) = f_\mathrm{e}(SOC_{\tau_\mathrm{e}}, I_{\tau_\mathrm{e}}, T_{\tau_\mathrm{e}}, V_{\tau_\mathrm{e}}, \dots) \tag{10}$$

with $SOC_{\tau_\mathrm{e}}, I_{\tau_\mathrm{e}}, T_{\tau_\mathrm{e}}, V_{\tau_\mathrm{e}}$ as time series of SOC, current I, temperature T or voltage V in the time window $\tau_\mathrm{e} = \left[t_\mathrm{past}, t_\mathrm{e}\right]$ that can either comprise a few cycles, a single cycle or less. Most importantly τ_e shall not cover any significant SOH change over time. The point in time t_e may be just now ($t_\mathrm{e} \leq t_1$). The electrochemical behavior expressed in the signals of SOC, I, T, and V changes due to battery aging [51]. Hence, SOH estimation is based on information that reflect the effect of battery ageing.

Second, we perceive battery ageing as a SOH state change $\Delta SOH(\tau_\mathrm{f})$ from a current $SOH(t_1)$ to a future $SOH(t_2)$ due to ageing causes. Predicting the future $SOH(t_2)$ given information on the current $SOH(t_1)$ and the battery operational load during the period of time $\tau_\mathrm{f} = [t_1, t_2]$ from now t_1 until the future point in time t_2:

$$SOH(t_2) = f_{\mathrm{f,I}}(SOH(t_1), SOC_{\tau_\mathrm{f}}, I_{\tau_\mathrm{f}}, T_{\tau_\mathrm{f}}) \tag{11}$$

with $SOC_{\tau_\mathrm{f}}, I_{\tau_\mathrm{f}}, T_{\tau_\mathrm{f}}$ as time series of SOC, I, T, and V in the time window τ_f that express the causes of the battery ageing due to battery operation explicitly. This ensures that the battery operational load is not implicitly considered to be fixed [52].

Alternatively, to the future $SOH(t_2)$ in Eq. (11) also the future change $\Delta SOH(\tau_\mathrm{f})$ can be forecasted:

$$\begin{aligned} \Delta SOH(\tau_\mathrm{f}) &= SOH(t_2) - SOH(t_1) = f_{\mathrm{f,II}}\left(SOH(t_1), SOC_{\tau_\mathrm{f}}, I_{\tau_\mathrm{f}}, T_{\tau_\mathrm{f}}\right) \\ &= f_{\mathrm{f,I}}\left(SOH(t_1), SOC_{\tau_\mathrm{f}}, I_{\tau_\mathrm{f}}, T_{\tau_\mathrm{f}}\right) - SOH(t_1) \end{aligned} \tag{12}$$

while learning the functions $f_{\mathrm{f,I}}$ or $f_{\mathrm{f,II}}$ in a regression model enables SOH forecasting. This is also called "future capacity prognostics by Liu et al. [53].

Summarizing, compared to SOH forecasting, SOH estimation does not model a change in state, but only a determination of state [54,55]. For SOH estimation, the time window τ is rather short and in the past, while it is longer and in the future for SOH forecasting. Furthermore, SOH estimation is based on data regarding the effect of battery ageing, while SOH forecasting is based on data regarding the causes of battery ageing. These distinguishing characteristics of SOH estimation and forecast are listed in Table 1.

Table 1: Distinguishing characteristics of SOH estimation and forecast

Distinguishing characteristic	Estimation	Forecast
Modeling	State determination	State change
Time window τ		
Length	Short	Long
Relative temporal position to t_1	In past	In future
$SOC_\tau, I_\tau, T_\tau, \ldots$		
Express information on	Electrochemical behavior	Applied load
Describe information regarding … of battery ageing	Effect	Causes

In the literature, apart from SOH estimation and SOH forecasting also the term SOH prediction is often used which seems ambiguous to SOH forecasting. In general, the terms "forecast" and "prediction" are in practice often used synonymously. However, dictionaries show slight differences in their definition [56–61], just as Petropoulos et al. [62] describe forecasting as prediction about the future. Cugh [63] and Döring [64] define forecast as prediction with temporal dimension.

We state that when having a SOH estimation model created based on past and present data, using this model to estimate a future SOH with unseen data from the future, this is called SOH prediction [64]. Hence, using SOH estimation models for prediction only enables observing the effect of battery ageing. For example, [65–70] create models using past and present data. To estimate the SOH they use features derived from the charging curves of current, voltage, and temperature. These curve changes are an effect caused by battery ageing. But they are hard to interpret and produce for humans. This means a user of the model, like a fleet manager, cannot derive changes of the charging curve (effect of ageing) from an assumed usage load of her BEV fleet (cause of ageing) with SOH estimation models – even when used for prediction. Only once the effect of battery ageing is observable in the future charging curve data, the model can predict the corresponding SOH. Thus, in advance no statement about a future SOH is possible with SOH estimation models. In contrast, SOH forecasting directly correlates causes of battery ageing encoded in battery operational time series data with their effect on the SOH.

2.1.2 State of Health vs. Remaining Useful Life

Another measure of the battery state is the RUL. According to Nuhic et al. [71] the RUL is defined as the number of charge-discharge cycles until a specific battery SOH is reached at EOL:[6]

$$RUL_{\text{EOL-SOH}}(t) = k(t_{\text{EOL-SOH}}) - k(t) \tag{13}$$

with k as number of cycles. The RUL usually refers to equivalent full cycles (EFC), but real-world operational battery cycles have different ΔSOC (Key criterion 1c in Table 2). In the operation of BEVs, the RUL can therefore only serve as an indicator for the number of potentially non-full cycles until the EOL. Usually for BEV batteries a SOH_C of 80 % is required which is defined as the end of life (EOL) of the first life (EOL-80) depicted as red line in Figure 2 [73]. Less common are 65 % and 50 % [74]. However, 80 % as EOL criterion is also questioned because of the increasing maximum capacity and, as a consequence, the increasing range of BEVs [75,76]. In reality, different BEV users may require different ranges leading to different EOL criteria.

[6] An alternative equation includes the current cycle in the RUL, i.e. RUL before the current cycle: $RUL_{\text{EOL-SOH}}(t) = k(t_{\text{EOL-SOH}}) - k(t) + 1$ [72].

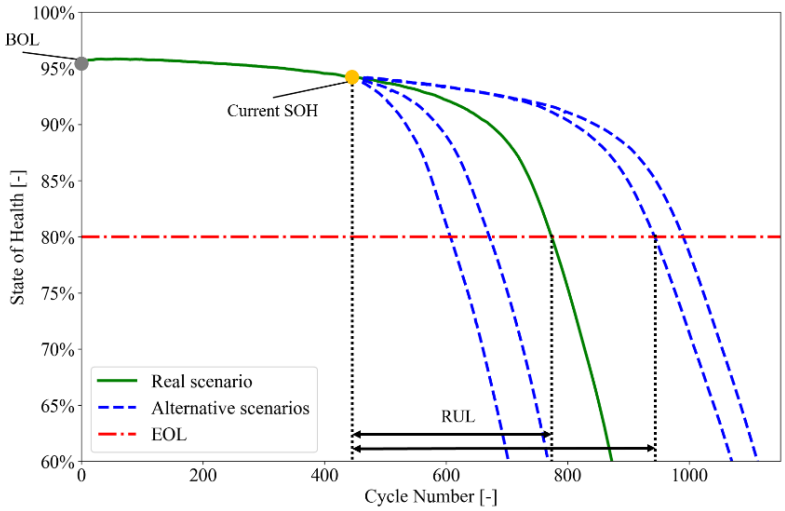

Figure 2: Relation of SOH and RUL with their different reference points to BOL and EOL respectively.[7]

Another EOL criterion could be the total lifetime of the battery [78]. EOL may be defined by a SOH_{R} of 200 % [31,79] or 160 % [35] when following the definition in Eq. (1). Also, the kneepoint is suggested as EOL criterion [52]. Hitting the EOL criterion does not imply that the battery cannot be used anymore, it only indicates that the predefined threshold has been surpassed [16]. In practice, manufacturers and users may define their own EOL criteria depending on their battery application [80]. They could related to the general concept of failure assessed by criteria like unsatisfying performance, incapable of providing certain functionality, and temporal availability [81,82].

SOH and RUL are connected as depicted in Figure 2: The SOH is describing the current battery state referring to the initial, new state at the BOL. Contrarily, RUL is describing the current battery state referring to the EOL of the battery. However, depending on the future load scenario applied to the battery the EOL is reached at a different point in time, as indicated by the dashed blue alternative scenarios in Figure 2.

Thus, in contrast to SOH estimation, for a RUL prediction, assumptions on the future load scenario need to be made. We observe two possibilities for these assumptions: First, the same load as in the past is assumed for the future like Gasper [83] does. In this case, SOH estimation has the same information as RUL prediction as the point in time when the EOL is reached is not variable for a single battery. Only the reference point for the state description and the unit are different: SOH in % refers to the BOL, while RUL in cycles refers to the EOL. Second, a different load in the future as in the past is assumed so that the RUL varies depending on the future load scenario (dashed blue lines). Thus, additional information about the future load is required by the RUL prediction model, contrarily to SOH estimation models. Under such assumptions SOH and RUL represent different information.

Tian et al. [9] point out, that "there is a strong connection between SOH and RUL" and state that "the SOH and the RUL can be estimated using the same methods […]." [9]. Considering the two presented cases regarding the future load compared to the past load, this statement holds only true for the 1st case. We see the 2nd case of RUL prediction comparable to SOH forecasting since the model requires information about the assumed future load.

Similar to [9], Ng et al. [33] state that to predict the "SOH [..] spanning many charge/discharge cycles" a function is necessary that "inputs the current state of the battery to predict future behavior" [33]. We argue that this is only partially true. As mentioned before, for the prediction of the future SOH, not only the current SOH has to be input but also information about the future battery load. Such information about the future load can only be ignored if a homogeneous load can be assumed. Just the same, Hu et al. [84] point out that a lack of missing future measurement results in RUL prediction errors.

[7] SOH data from batteries no. 15, 16, 38, 43, 45 of the 4th batch from [77].

Dealing with uncertainty becomes even more important when switching from laboratory to real-world data [54]. Since we focus on the input features of the model in this survey and its transferability (Key criterion 1 and 2 in Table 2), uncertainty can be considered when choosing a machine learning model.

In both discussed cases, a RUL prediction model only predicts the number of cycles to a single SOH like EOL_{80}, so several RUL prediction models would be required depending on the SOH of interest. However, a single SOH model can forecast a range of SOHs. This is relevant for BEV fleet operation and also 2nd life applications, as batteries in the 2nd life application usually have a lower SOH (Key criterion 1c & 3), for which a RUL prediction model of the 1st life would not be applicable. Additionally, the transition from 1st to 2nd life application is smooth and not necessarily bound to a fixed SOH like 80 %. This raises the question which output values are appropriate for a RUL prediction model after EOL. Negative values may indicate how many cycles a battery is past the EOL criterion.

A SOH forecasting model can still be used to obtain the RUL: The inputs of the SOH forecasting models contain direct or indirect information on the number of cycles operated. Under this assumption, the inputs can be adapted until e.g. EOL_{80} is reached similar to the procedure of Lui et al. [85]. Alternatively, the forecasted SOH can be compared with the EOL threshold like 80 %, similar to the procedure of Deng et al. [86]. If the forecasted SOH is greater than the EOL threshold, the RUL is positive. Otherwise, the EOL has been reached already. From this point of view, SOH forecasting can be seen as a generalization of RUL prediction.

Still, any model applied in the 2nd life has most likely to consider different operation conditions than a model applied in the 1st life. For example, grid applications as 2nd life application are typically more favorable regarding battery aging because of their thermal management systems, reduced SOC windows, and C-rates compared to EVs as 1st life application [54].

Which measure of SOH and RUL to favor, depends on the objective and application of the model's user. If a user has a sense for the quantity of cycles her batteries are loaded per week, RUL may be a suitable measure to temporally classify when the batteries are going to reach the defined EOL. Contrarily, if no specific SOH is defined as EOL threshold, the SOH may be the favorable measure as it can be linked to technical specifications like a minimum required capacity for a certain battery application or a minimum required range of a BEV. Additionally, the residual value (RV) of a BEV's battery is linked to offered range, i.e. capacity [87]. Thus, SOH is favorable to indicate RV as well. Additionally, for the transition from 1st to 2nd life application of the battery the SOH as continuous measure is more suitable.

2.2 Model Key Criteria

Inspired by the applicability from a user's perspective of BEV fleet managers and battery designers we motivate and define the following key criteria of a model for SOH forecasting. These key criteria are extended from our own prior work [88] and summarized in Table 2.

Table 2: Key criteria for a SOH forecasting model

Key criterion No.		Key criterion description
1a	Model inputs	- Contain information about the future load
1b		- Information about future load is aggregated
1c		- Capture the higher variability of real-world battery operation compared to laboratory operation
2	Transfer to new batteries	
3	Applicable for 2nd life applications of batteries	

Key criterion 1a: Assuming a certain load scenario of a BEV fleet, the fleet manager is interested in the future SOH of the fleet's vehicles. The usage load can vary for example due to the charging strategy. This means the decision to prefer AC or DC charging, i.e. using either the vehicle's onboard inverter or the AC-to-DC rectifier of the charging station before reaching the vehicle's battery, bypassing any onboard inverter. For the fleet manager it will not be valid to assume the same load in the future as in

the past. Thus, for our survey we require models to have explicit information about the future load as model input (Key criterion 1a).

This is coherent with the literature: Lucu et al. [17] note that batteries in real-world operation, e.g. in automotive applications, exhibit varying loads during the battery's lifetime. Furthermore, [83,89–91] assume that future battery degradation is independent of the battery's past history. Therefore, information about the future operating load of the battery is essential for SOH forecasting.

Fulfilling this key criterion shall enable a model to output future SOH fade or the future SOH based on the current SOH and future load like Lin et al. [92] point out similarly. Furthermore, in real-world operation batteries age slowly so the relevant multidimensional time series contain years of operational data at a milliseconds sample rate [88]. This temporal scale requires some data aggregation or compression and complicates satisfying key criterion 1a.

Key criterion 1b: When applying the SOH forecasting model in production, explicit information about the future load is required (Key criterion 1a). The future battery load is determined by multidimensional time series of temperature, current and SOC. The United States Advanced Battery Consortium set the development objective for battery life of 15 years and 1000 cycles [93]. This means in real-world operation batteries age slowly, so the relevant time series contain weeks or months of operational data. Furthermore, the sampling rate should be in the range of seconds or milliseconds to capture relevant operational dynamics, e.g. different acceleration profiles in city traffic.

First, for forecasting into the future no data from the future battery load is available in the present. Thus, a human needs to express her assumption on the future load via the model's input [94]. Such assumptions can for example regard the charging policy, preferred rest SOC, and limitations of the SOC operating range. Though, the data of the future battery load is composed of long and multidimensional time series which are difficult to interpret and produce by a human [95].

Second, in vehicle fleet operation cost reduction is critical for profitability. This also includes costs due to logging operational data of the vehicle fleet as well as transmitting and storing the data e.g. in a cloud. Nuhic et al. [71], Nuhic et al. [96], and von Bülow et al. [88] identify this as a central challenge when forecasting the SOH. Contrarily to these cost factors, computational cost for SOH forecasting is likely to be negligible compared to running edge computing in the BEVs, if it is provided as a data-driven fleet service in a cloud system [97].

Third, the input data of an SOH forecasting model needs to be compatible with the underlying method, e.g. a machine learning model. The described time series are too long and finely sampled so that e.g. a recurrent neural network (RNN) would suffer from vanishing gradients [98,99].

These three problems regarding the data of the future battery load can be solve by data aggregation and feature extraction (Key criterion 1b). This is a common procedure with long time series in general, e.g. in the domain of machine health forecasting [100–103]. Further, it enables humans to run what-if-simulation with the SOH forecasting model.

Existing approaches like the one from Song et al. [69] for SOH estimation require data of future charging cycles for prediction like the charging curve of current, voltage and temperature. These time series change when the battery ages but are hard to interpret for humans. This means a user of the model, like a fleet manager, cannot derivate changes of the charging curve from an imagined usage scenario of her BEV fleet. The same applies to the work of Liu et al. [104] who use the incremental capacity (IC) and differential voltage (DV) curves as forecasting inputs.

Key criterion 1c: BEV fleet managers and battery designers are not only interested in battery ageing in laboratory experiments, but especially keen on forecasting battery ageing in real-world applications. However, as described in Section 2.3 the common load of batteries in laboratory and real-world operation differs, e.g. regarding charging and discharging current, temperature, and ΔSOC. Overall, data from real-world operation is more complex and variable than laboratory operation. Thus, the model's inputs about the future load shall be able to capture the higher variability of data from real-world battery

operation compared to laboratory operation (Key criterion 1c). This is also pointed out by several authors [84,94,95,105–112].

Key criterion 2: When launching a new battery type, e.g. with a new cell chemistry, a reliable model for SOH forecasting suitable for the new battery type is required quickly to support established services. Nevertheless, the available amount of data of a new battery type is limited in the initial phase. Extensive data generation as solution is expensive and difficult as battery ageing is a lengthy process. Data synthesis or augmentation from physical ageing models still needs validation from laboratory tests. Furthermore, we consider an adaption of feature values of ageing data and knowing the resulting ageing as too difficult. The complexity of this causal relationship is the main reason why data-driven models are considered for SOH forecasting. Another solution is to transfer an established model for battery ageing of another battery type to the new battery type, as soon as a small amount of data of the new battery type has been gathered [97,113]. Thus, the required amount of data shall be minimal at least once an initial model has been trained so that it can be transferred easily to new batteries (Key criterion 2). Transferability of models to new cells is also mentioned as desirable by Li et al. [105] and Shen et al. [114].

A method suitable for satisfying this key criterion is called transfer learning and has been successfully applied in other domains like computer vision [115]. The application of transfer learning for battery SOH forecasting models is a crucial part, as there are differences in battery systems like the nominal capacity, the cell anode and cathode materials as well as the applied load due to usage. However, the general electrochemical behavior of lithium-ion batteries is a major common characteristic which provides an excellent starting point for transfer learning.

Key criterion 3: Once batteries in automotive applications are not satisfactory anymore, e.g. regarding capacity or performance desired by the user, they shall be reused in 2nd life applications. Such 2nd life applications like stationary energy storage for grid stabilization usually have less demanding performance key criteria so that older batteries are still suitable. In automotive applications a SOH of 80 % is often mentioned as threshold for the transition to the 2nd life application [73,116]. However, manufacturers, fleet managers, and users may choose a different EOL criterion, as pointed out in Section 2.1.2. Also, from a data point of view separate models are debatable: Separating data into two models that include the same ageing mechanisms as lithium plating that become more dominant towards the end of 1st life would be a drawback for both models. Hence, the model shall be continuously applicable to the 2nd life application of batteries as well, i.e. below a SOH of 80 % (Key criterion 3). This means the model shall be capable of covering the knee point, when new ageing mechanisms like lithium plating become dominant and accelerate ageing [117]. Thus, the knee point is important to learn for SOH forecasting models. However, SOH trajectories not always show a knee point. For further information consult [118].

When concerned about vehicle replacement, BEV fleet managers are less interested in the SOH forecast after a single cycle or a week, but after some weeks or months once the batteries have aged significantly. Thus, we also examine the forecast horizon of SOH forecasting models, but do not define an additional key criterion therefore.

Most SOH forecasting methods are providing one-step forecasts, only few output multi-step[8] forecasts [119]. If a SOH forecasting model executes a one-step forecast, multi-step forecasts can be realized by recursive stepwise forecasting as proposed by Liu et al. [120] and Falco et al. [121]. Nevertheless, this increases the prediction error due to error propagation. Also, Falco et al. [121] mention that the lead time increases. Furthermore, Liu et al. [122] point out that k-steps-ahead forecasts with large k „cannot obtain satisfactory results“ using a Gaussian process regression (GPR) model, also shown by Shi et al. [123]. Hence, multi-step forecasting models are preferable.

[8] These are also called one-step-ahead or single step forecast in contrast to m-step-ahead or m-step forecast.

Intrinsic cell-to-cell variability is caused by manufacturing differences, e.g. due to fouling [105,124,125]. However, it cannot be influenced by battery operation, but can be seen as a boundary condition for SOH forecasting that needs to be learnt.

2.3 Laboratory vs. real-world battery operation

Section 2.2 introduced key criterion 1c that the inputs of a SOH forecasting model shall "capture the higher variability of real-world battery operation compared to laboratory operation". This Section elaborates in more detail on the differences of real-world battery operation compared to laboratory operation [83].

When conducting battery ageing experiments in the laboratory like in the public datasets presented by [77,126–129], usually a test matrix specifies the controlled operation conditions relevant for battery ageing during the operation modes charging, discharging, and rest of the batteries. When considering a cycle of charging and discharging, the SOC lift (ΔSOC) as well as possible recuperation need to be defined as well. Furthermore, during all three operation modes the ambient temperature is relevant. These criteria in Table 3 show that laboratory operation of batteries usually differs significantly from battery data from real-world operation of BEVs since test matrices cannot completely cover the realistic operating conditions [54,71,109,130].

Table 3: Differences of laboratory and real-world operation of batteries

Ageing	Criterion	Laboratory operation	Real-world operation of BEVs
Cyclic	Charging	CC-CV or Multiple CC-steps, then CV	Similar to laboratory, but variable duration, current drops, and possible current limitations
	Discharging	CC or Randomized	Highly variable current
	Recuperation	None	Yes
	ΔSOC	100 % or other constant value	Highly variable
Calendar	Hold/Rest/Storage	Non or only short or solely for calendar ageing experiments	Dominant operation mode
Cyclic & calendar	Temperature	Constant room temperature or in temperature chamber without cooling system	Variable, depending on season, but with cooling system

In laboratory operation batteries are usually fully charged applying the constant current constant voltage (CC-CV) protocol [126,128]. Some datasets also have multiple CC-steps before the CV-phase [77,129]. In the real world, a chosen charging protocol may be facing current drops, when additional BEVs are starting charging at the same charging station and power supply is limited. Also, the charging management may limit the charging current depending on the battery's temperature. Furthermore, BEV batteries are not always fully charged. Especially, when applying fast-charging at highways the CV-phase is usually skipped [131].

In laboratory operation batteries are usually discharged using a single CC-step [77,127–129]. Only one public dataset applies multiple CC-steps of 5 minutes length with randomized discharge currents [126]. However, in real world application the discharge current is not constant, but highly variable, non-linear and contains huge, but brief power demands [18].

Due to regenerative braking, i.e. recuperation, in automotive applications charging and discharging mode alternate frequently, especially when driving in urban areas [18]. From a battery point of view,

recuperation can be seen as micro-charging during a longer discharging process which is also called partial or micro cycling. This is usually not considered by test matrices of laboratory operation.

Fully charging and discharging, i.e. $\Delta SOC = 100\ \%$ is common in laboratory operation [77,127,128]. Alternatively, the SOC_{start} and SOC_{end} of each cycle are constant so that $\Delta SOC = const.$ [129]. However, in real world application, ΔSOC of cycles are highly variable [131].

Furthermore, BEVs usually do not use low SOCs frequently due to the range anxiety of the drivers [132,133]. However, in HEV the complete range of the SOC is used. The same applies for BESS. These can be used for the optimization of own consumption (private and commercial), peak shaving, and frequency regulation (primary control) [134]. Corresponding markets are the frequency containment reserve (FCR), intraday continuous market, and day-ahead auction market [135]. Compared to automotive high voltage (HV) battery applications, batteries in BESS applications have around 3 full cycles per day [7,136].

If calendar ageing is not examined in laboratory operation, rest phases without any current applied are usually temporally negligible compared to the duration of charging and discharging phases. Usually, they are only part of the experiments, e.g. for voltage relaxation and characterization tests. However, in standard automotive and BEV use cases rest phases, i.e. inactive HV system and open HV contactors, are usually dominant [18,137]. Even if the BEV is not moving, some current is always applied for auxiliary consumers, like air conditioning and entertainment system. Only, in MaaS use cases of BEVs rest phase are less dominant because the vehicles are operated more intensively [23].

In laboratory operation batteries are usually exposed to a constant ambient temperature which is either the room temperature or forced by heating/cooling chamber [138]. In contrast, batteries operated in automotive applications face the complete seasonal range of temperatures from a cold winter night to a hot summer noon, especially when parked outside. Batteries operated in BESS usually have better thermal environment conditions than in automotive applications.

3 Screening Method

We conducted our literature review following Webster and Watson [139]. We used Web of Science [140] and Bielefeld Academic Search Engine (BASE) [141] to find relevant articles for this survey. Web of Science searches in relevant journals and conferences in the field of energy storage and batteries. Because Web of Science does not include open-source publications, we looked in BASE for papers which are not duplicates with the Web of Science search. Using Google Scholar [142] we found approximately 18,500 papers. A sample analysis showed that over 90 % of the papers found were categorized as irrelevant only based on the title. Thus, we opted against the use of Google Scholar because too many irrelevant papers were found and reproducibility is highly limited. Additionally, it also does not enable the mass export of bibliography information and the length of the search string is limited to 208 characters. Lastly, we also did not include semantic scholar [143], as it does not enable searching with Boolean operators.

This review is conducted based on content analysis. We defined keywords for the search string and then looked for synonyms of these keywords as depicted in Table 4. This review focuses on lithium-ion batteries. Still, we want to include methods developed for other battery type because they may be applicable and relevant to lithium-ion batteries. As pointed out in Section 1 and 2.1, SOH prediction and forecasting are not clearly distinguishable in the literature. Additionally, the terms “predict” and “forecast” are often used synonymously [58]. Thus, we considered both. As explained in Section 2.1, RUL and SOH can provide similar information. Also, as defined in Eq. (2) the SOH is the relative capacity. Thus, we classified these terms as synonyms. No keyword like method, model, equation, machine learning model or the like is chosen because we are reviewing data-oriented and method-neutral, not method-oriented like others surveys [14,17]. We did not limit the search by a certain time like “only publications published from 2015 to 2022”.

This resulted in the following search string: (“battery” OR “batteries”) AND (“Ageing” OR “aging” OR “Degradation” OR “Deterioration” OR “Capacity fade” OR “Capacity loss”) AND (“Forecast” OR

"Forecasting" OR "Prediction" OR "Predict" OR "Predicting" OR "Prognostics") AND ("State of Health" OR "Capacity" OR "Remaining Useful Lifetime" OR "Remaining Useful Life").[9]

Table 4: Keywords and synonyms for the literature review. Synonyms are connected with the keyword by OR-operator.

Keyword	Battery	Ageing	Forecast	State of Health
	Batteries	Aging	Forecasting	Capacity
		Degradation	Prediction	Remaining useful lifetime
Synonyms		Deterioration	Predict	Remaining useful life
		Capacity fade	Predicting	
		Capacity loss	Prognostics	

The filtering process of 2017 papers from our initial search is depicted in Figure 3. Based on the defined criteria in Table 2, we filtered 1045 papers by title, 389 papers by abstract, and 521 papers by the full text from the initial 2017 papers. Many papers filtered out were about either the estimation of SOH and SOC or investigating battery ageing mechanisms. Hence, 62 papers remained for which we executed a forward and backward search according to vom Brocke et al. [144] which resulted in six and respectively three added papers. The extended corpus of 71 papers was split into 51 research publications, 15 relevant review papers, and five perspective papers. The selected 51 research papers were read carefully regarding the key criteria for SOH forecasting models defined in Table 2 in Section 2.2. As listed in Table 7 in the Appendix, out of the 51 research publications 80 % were journal articles while each 10 % were conference papers, and published online, e.g. as PhD thesis on university publication servers (3). The most common Journals were the Journal of Power Sources (16 %) and the Journal of Energy Storage (16 %). The papers are spanning from 2010 onwards, with over 65 % of the papers published from 2020 onwards.

[9] Web of Science: Searched using topic which includes the fields title, abstract, author keywords, and Keywords Plus. BASE: Searched using title and subject headings. For searching in BASE the search string was adapted by removing all OR-operators and the quotation marks if the keyword or synonym consisted of a single word: (battery batteries) AND (Ageing aging Degradation Deterioration "Capacity fade" "Capacity Loss") AND (Forecast Forecasting Prediction Predict Predicting Prognostics) AND ("State of Health" Capacity "Remaining Useful Lifetime" "Remaining Useful Life")

Figure 3: Overview of papers found by database (dated: 13.10.2022)

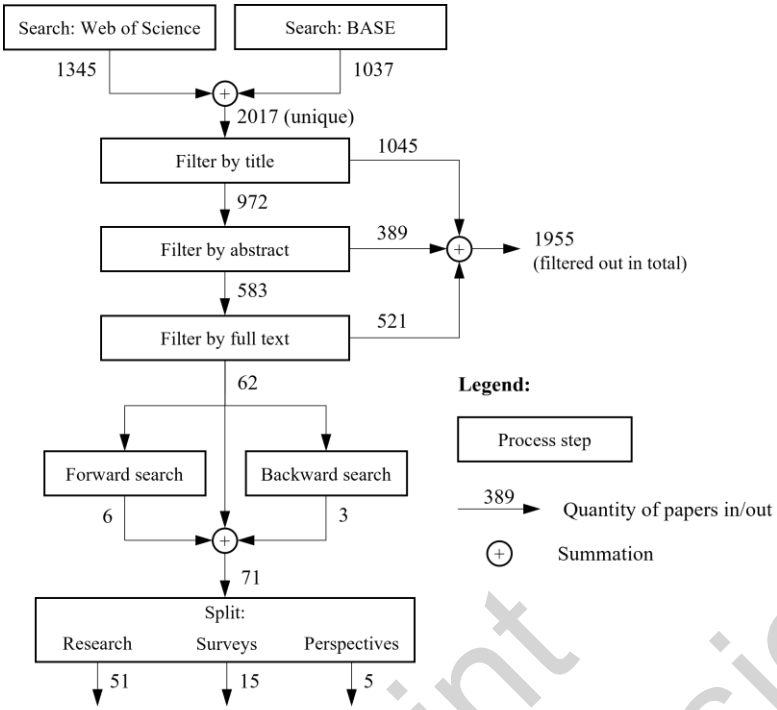

4 SOH Forecasting Models

When filtering the 2017 initially found papers by title, abstract, and full text, we identified certain categories of models as fundamentally unsuitable regarding the key criteria defined in Table 2. Afterwards we structure and present the relevant models. The unsuitable models are summarized in the following:

There exist many papers [90,145–156] that present physical, empirical, or semi-empirical models or derive equations for describing battery ageing. These models provide a very good indication which operating condition accelerate battery ageing. However, these models are based on laboratory experiments executed under controlled conditions in which each ideal cell is linked statically to a specific operation protocol until EOL [157]. In each operational protocol only one or a few operational parameters vary. This limits the model application in real-world operation when multiple operational parameters vary dynamically over several batteries [158,159] (Key criterion 1). Karger et al. [160] propose an empirical model with non-global power exponents considering switching operational load after every 100 EFC, but still no explicit input of the operational load is given to their model. Because of the open-loop nature of these models, their generalization and adaptability particularly in long-term predictions is limited [120].

For SOH estimation the ECM has been discussed by Barré et al. [161]. However, Ng et al. [33] point out that even though computational efficient, ECMs show limited prediction accuracy across operation conditions in real-life applications that are different to laboratory conditions. Additionally, the difference of SOH estimation and forecasting needs to be considered as described in Section 2.1.

Many papers apply particle filters to predict the SOH trajectory, i.e. to predict future battery ageing. Less common is the Kalman filter [17]. Both are empirical parametric ageing models that recursively update their parameters every time new data is available (update step) and estimate the current state (predict step) [162]. However, estimating a future state would require assumptions on feasible measurement variables. In their review, Lucu et al. [17] list solely models with capacity or internal resistance as measurement variable which are the state variables of interest. So, these approaches are just autoregressive. Autoregressive[10] models output the SOH based on past SOH values [105,122,163–

[10] Hu et al. [84] describe autoregressive models as having an “iterative structure”.

168]. This still prohibits SOH forecasting into the far future. Also, no explicit information about the future load is input of these models (Key criterion 1a). Thus, these models assume the same load in the future as in the past. However, batteries cycled in real-world operation, for example in automotive applications, may have a varying load over the life of the battery. Furthermore, most autoregressive models only do one-step predictions.

The relevant models found in this survey were hierarchically structured in four groups visualized in Figure 4 regarding the model's input information of the future battery load. These four groups of models are: Those without information about future load often have only the number of cycles k or the charge throughput Q_{thrpt} in ΔAh as input (Section 4.1). Those with information about future load have either no distributional information (Section 4.2.1) or distributional information. Distributional information about future load refers to information, e.g. about the distribution of the charging current. This enables encoding the variability of real-world battery operational data in the model's inputs (Key criterion 1c). Models with distributional information about future load can either include rainflow counting or only histograms (Section 4.2.2.1 or 4.2.2.2 respectively). The models presented in each of the mentioned subsections are also summarized in Table 6. In each subsection we first give a general introduction and then present the works from Table 6 in more detail.

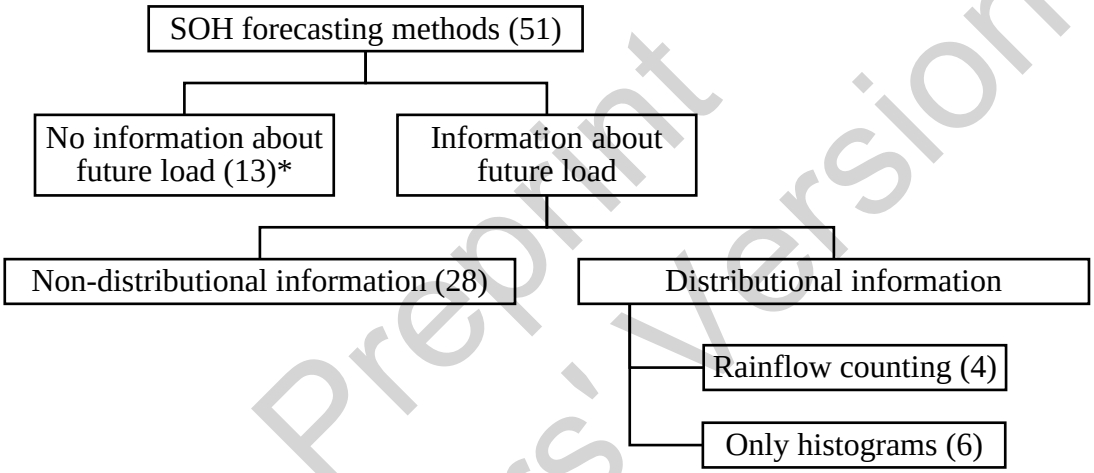

Figure 4: Structure of SOH forecasting methods regarding the methods' input information about future battery load. Number of papers in brackets. *These 13 papers are representative for this category that includes papers describing physical, empirical, semi-empirical, autoregressive, or equivalent circuit models (ECM). These methods do not fulfil key criterion 1a because they do not have any information about future load.

In the context of this review, no uniform symbology has been identified in the paper corpus. To increase comparability, readability, and comprehensibility across paper boundaries, we introduce and use the uniform symbology listed in Table 5.

Table 5: Explanation of features identified in this survey with according symbols

Symbol	Explanation	Symbol used in other papers
k	Number of cycles	n
t_1 and t_2	Beginning and end of time period	
$\Delta t = t_2 - t_1$	Time span from t_1 to t_2	d
C	Capacity	Q, $q_{\max}$
ΔC	Capacity loss	ΔQ
R_i	Internal resistance	IR, R, R_0
SOH	State of Health or relative capacity	SoH, RC
ΔSOH	Change/ loss of SOH or relative capacity	RCL
SOC	State of Charge	SoC
$\emptyset SOC$	Middle SOC or average SOC	$\overline{SOC}$
$\Delta SOC = \max(SOC) - \min(SOC)$	SOC lift or SOC-swing (SOC-S)	$SOC\text{-}S$
$SOC\text{-}SR = [SOC(t_1), SOC(t_2)]$	SOC swing rate	
$DOD = 1 - SOC$	Depth of Discharge	DoD
Q_{thrpt}	Charge throughput in ΔAh	
T	Temperature	
T_{rest}	Rest, hold, or storage temperature	T_{storage}
T_{ambient}	Ambient temperature	
I	C-rate or current	
V	Voltage	
P	Power	

In Table 6, we also list the open-source availability of code and data which increase the understanding of the presented methods and allow an easier comparison to other models and other data. As overfitting is a problem in the domain of machine learning and modeling, we check whether authors dealt with overfitting, e.g. by data splitting or cross-validation [169]. The fulfillment of key criteria 1a-c is dependent on the model's inputs. The vast majority of the found models is applied to lithium-ion batteries, other batteries types like lead-acid batteries [170] are not so much in focus of research regarding SOH forecasting.

As observable in the Table 6, only a few public data sets were used in the reviewed papers. More than half of the authors generated data themselves and did not publish it afterwards (60 %), which means that the comparability and verifiability as well as the possibility for further use of the results are not given. As dos Reis et al. [171] and Naaz et al. [172] state this is a common problem in the domain of battery models. Also, the code is only rarely shared (10 %). A broad range of metrics to measure the models' performance is used. The most used are root mean squared error (RMSE, 37 %), mean squared error (MSE, 6 %), mean average error (MAE, 14 %), and mean absolute percentage error (MAPE, 12 %). The most frequently used output values are C (35 %), ΔC (29 %), and SOH (16 %). RUL is only used in 12 % of the identified models. Additionally, the forecast horizon of the models is often difficult to interpret and not explicitly given in the reviewed papers. It is measured differently, e.g. in cycles, days or Ah. Usage of different data sets, different metrics, different output values, and different forecast horizons complicates the comparability of the models' performance. Regarding different metrics, Ochella et al. [173] point out the importance of their standardization as well.

In this survey, machine learning models were the most used (71 %). Due to the variability of the inputs and complexity of the data, the machine learning models are easier able to find patterns and rules in the data than manually defining e.g. an empirical model. Among the machine learning models GPR was the most popular (31 %). Overfitting is not checked by all authors (only 49 %). This is problematic because after fitting models need to generalize well on unseen data. The forecast horizon of the models

is diverse including models forecasting a single cycle, several cycles or several days. In most papers, the forecast horizon seems to depend on the interval of SOH measurements in the used data.

The majority of the five chosen key criteria is only satisfied by a few methods. All key criteria are only satisfied by von Bülow et al. [88] with model transferability shown in [174] (Key criterion 2). It has to be noted that the key criteria for this review are extended from von Bülow et al. [88]. The models without information about the future load satisfy either key criterion 1a or 1b, but fail at satisfying both. The models with non-distributional information satisfy key criteria 1a and 1b, but fail at key criterion 1c. Only the models with distributional information satisfy key criteria 1a and 1b. Transferability of SOH forecasting has not yet been shown with GPR, but with MLP based on their layer-wise architecture [174] (Key criterion 2). Given the popularity of GPR applied to SOH forecasting, transfer learning with GPR in this field needs further research. If the RUL or cycle life is not used, but SOH or capacity is used as output value, the model is applicable to 2nd life applications (Key criterion 3). So this key criterion is easy to satisfy.

4.1 Models without information about future load

Models without information about future load do not have model inputs regarding the operational conditions I, SOC, and T of the battery in the future (Key criterion 1a). They often only have the time t passed, the cycle number k[11] or the amount of charge throughput Q_{thrpt} as inputs. However, Lucu et al. [17] see such simple SOH forecasting models as "debatable for Li-ion battery ageing modelling" [17]. The models of this category from Table 6 are presented in this Section.

Richardson et al. [91] apply GPR with the cycle number k as input to output the corresponding SOH. The authors note that future work may include DOD, T, and t_{rest} as inputs which are missing in this work.

Tang et al. [175] use MATLAB's nonlinear curve fitting algorithm to fit the relation of the cycle number k and the SOH with a piecewise cubic interpolation function. When using 30 % of the SOH curve for fitting, a prediction RMSE of 2.5 % is reached.

Semanjski and Gautama [176] fit the SOH using a linear function with k as single input. Their assumption of linear ageing can cause errors, given the potential non-linearity of SOH trajectories. They used real-world ageing trajectories, but information about the battery operation is ignored as model input (Key criterion 1a).

Guo et al. [177] develop a Bayesian approach for capacity fade modeling. However, the number of cycles is the only covariate. Also, they only perform one-step-ahead predictions.

Severson et al. [127] investigate features derived from the discharge voltage curves from the first 100 cycles to predict the cycle life with an elastic net. Their features are too complex to be human-producible and interpretable (Key criterion 1b). Furthermore, no information about the future load is input of the model (Key criterion 1a).

Attia et al. [178] build on the model from Severson et al. [127] as base line. Attia et al. [178] again use features from the voltage curves, but try to compactly represent them and reduce the voltage sampling frequency. The model still does not fulfil key criteria 1a and 1b.

Li et al. [105] train an long short-term memory (LSTM), with the capacity history until the present point in time which outputs the future trajectory until EOL. In further work, Li et al. [168] add input and output data of the internal resistance training a multi-task learning (MTL) RNN. However, both models are autoregressive so that no explicit information about the future load is input of the model (Key criterion 1a).

Giorgiani do Nascimento [179] proposes to learn the battery capacity C from the cumulative energy E using variational MLPs (vMLPs) [180]. In vMLPs deterministic weights and bias are replace by normal distributions. The vMLP uses elu as activation function and only has 3 layers with 4, 2, and 1 neuron

[11] Hu et al. [84] describe the structure of such models with $C = f(k)$ as "non-iterative".

respectively. Giorgiani do Nascimento [179] mention as an advantage of their chosen input that both constant and randomized discharge data can be used. However, both can not be further distinguished by the model. The author does not provide a performance metric of the final model.

4.2 Models with information about future load

In this Section, models are presented that have information about the future battery load as input (Key criterion 1a). First, models without distributional information, second models with distributional information as model inputs are presented.

4.2.1 Models without distributional information about future load

The models in this Section only partially satisfy key criterion 1c because of the variability of operational load in real-world which makes distributional information of the operational load necessary. I.e. giving a constant or the mean discharge current of a time window does not provide information about the distribution of discharge current over time.

Lucu et al. [181] propose a GPR model for calendar ageing which outputs the capacity loss ΔC with the rest time Δt_{rest}, reciprocal of the temperature T^{-1} and the SOC as inputs, where the last two features correspond to the rest time. The model is only considering calendar ageing. Furthermore, the inputs are not suitable to capture the variation of real-world operation (Key criterion 1c) because no distributional information of T^{-1} and SOC are given to the model.

In further work, Lucu et al. [182] dissect a GPR model for cyclic ageing which outputs the capacity loss ΔC with Q_{thrpt}, reciprocal of the temperature T^{-1}, DOD, the Middle-SOC ($\emptyset SOC$), charging, and discharging C-rate as inputs. All features except Q_{thrpt} are corresponding to the cycled Q_{thrpt} in ΔAh. The model is only considering cyclic ageing. Furthermore, the inputs are not suitable to capture the variation of real-world operation (Key criterion 1c) because no distributional information of T^{-1}, DOD, SOC, charging, and discharging C-rate are given to the model.

Lucu et al. [183] combine their previous works [181,182] to learn progressively from realistic EV driving data, starting from laboratory data. With realistic EV driving data the model's predictions improve. As [183] note their model cannot capture the "dynamic character of the DOD stress factor's profiles, which may induce lower ageing rates compared to the static DOD ageing profiles", which only had 20 %, 65 %, and 100 % DOD. Thus, this model still does not fulfil key criterion 1c.

Andre et al. [184] use support-vector regression (SVR), to learn the relative capacity which is the $SOH(t_2)$ based on the following inputs: $SOH(t_1)$, T_{min}, T_{max}, time span $\Delta t = t_2 - t_1$, I_{mean}, $Q_{\mathrm{thrpt,charge/discharge}}$, SOC_{max}, and ΔSOC. They only state the max. error of 20 %; information on other metrics like the RMSE is not given. When comparing Figure 9a) and b) in [184] some overfitting can be assumed. There is no explicit information that overfitting has been tried to avoid.

Barré et al. [161] predict the capacity based on output energy, I sign alternation, distance, T_{storage}, and $t_{\mathrm{experimental}}$ in d. They use Least Angle Regression (LARS), ridge regression, Last Absolute Shrinkage and Selection Operator (lasso), and elastic net as regression models. Due to the feature "distance" the model seems not applicable to stationary 2nd life applications (Key criterion 3). The results are also limited because only data of a single battery is used. The battery has only been used for 45,038 km, 1,687 cycles, and 13,077 kWh resulting in a final SOH of 86.5 %. Furthermore, the capacity prediction is only executed after the end of a session, e.g. a driving session starting with 5,714 km and ending with 10,318 km.

Liu et al. [120] recognize that Richardson et al. [91] do not consider different T and DOD, while another work of Richardson et al. [185] only did not consider different DOD levels. Thus, based on the later work of Richardson et al. [185], Liu et al. [120] present a GPR model with the current battery capacity $C(t_1)$, optionally the past battery capacity,[12] the ambient temperature T_{ambient}, and the DOD as inputs. Like Richardson et al. [185], their model outputs the capacity one cycle later. For k-multistep prediction

[12] $C(t-i), \dots, C(t)$ with $i = 0, \dots, 4$.

they propose a recursive process of k single step predictions by replacing the model's current and past battery capacity stepwise with the new predicted capacity. However, compared to single cycle prediction the RMSE of the multistep prediction increases by 46 % in the best hyperparameter configuration. They do not use information on the SOC, as the $\emptyset SOC$ was 50 %, but only the DOD was varied. Furthermore, no distributional information of T_{ambient} and the DOD are considered.

Liu et al. [186] propose a LSTM calendar ageing model for $C(t+\Delta t)$ with $C(t)$, Δt, SOC_{storage}, and T_{storage} as inputs. Transferring their base model is successful with a RMSE of 0.0064. Methodically, the output layer from a trained LSTM base model is removed and new layers are added which then are trained on little data from unseen storage conditions of interest. Applying the method to cyclic ageing is still open.

Rohr et al. [187] suggest three event-counter features which act as stress factors for lithium plating. These features are counting the events of 1) high I_{charge}, 2) high I_{charge} & low T, and 3) high I_{charge} & high DOD. Neither do they specify what "high" means for the three signals nor is discharging information included. Their work only proposes features concerning cyclic ageing and charging for SOH forecasting but does not apply them on a data set or model.

Salucci et al. [188] present a Multivariable Fractional Polynomial (MFP) based on inputs obtained from the discharging cycles and $C(k)$ to output $\Delta C(k+m)$ which is m cycles later. The forecast horizon m is defined by two consecutive reference cycles, which correspond to 50 discharge cycles. Their inputs obtained from the discharging cycles are: the average of the minimum and maximum T $\overline{T_{\mathrm{min}}}$ and $\overline{T_{\mathrm{max}}}$, the average current $\bar{I}$, the cycle duration Δt from cycle k to $k+m$, the fraction of short cycles λ_{short} within the forecast horizon m, the rest time Δt_{rest}, the average initial voltage $\overline{V_0}$, the voltage difference of the discharge cycle $\overline{\Delta V}$, and the average of a rough capacity estimation at each discharge cycle during the forecast horizon $\overline{C_{\mathrm{approx}}}$. The use of $\overline{C_{\mathrm{approx}}}$ is problematic because it contains information about the development of C during the forecasting horizon. Also, the use of information about V might be less intuitive than information about SOC, e.g. for fleet managers without a battery technology background. Information from charging is not input of the model because only CC charging is used in the NASA Randomized Battery Usage Data Set so the model would require adaption for real-world data (Key criterion 1c).

Hosen et al. [189] introduce a model with k, charge and discharge I & T, T_{storage} and SOC_{storage} as seven inputs and $C(k)$ as output. They examine ensemble-bagged trees, GPR, SVM, and linear regression as machine learning methods, finding GPR as best with an RMSE of 0.2956. They do not consider distributional information of any I, T, or SOC which would be important for real-world application (Key criterion 1c).

Aitio and Howey [170] use GPR to predict the EOL defined by SOH_{R} for 1027 solar off-grid lead-acid batteries. They use the $R_{\mathrm{i}}(t)$, $\frac{\partial R_{\mathrm{i}}(t)}{\partial t}$, calendar age, Q_{thrpt}, k, cumulative time spent at float charge, $\bar{T}$, and $\bar{V}$ as features to predict EOL 0-8 weeks in advance. Their work is one of few directed at SOH_{R}, but uses similar features as the others which forecast the SOH_{C}.

Micari et al. [190] demonstrate the usage of an empirical model charge & discharge I, T, and DOD as inputs. The model outputs the capacity drop $\Delta C(t)$ after one second. Compared to the relevant time frame of battery aging of weeks or months for practitioners, a one-second-forecast indicates that the model needs adaption.

Safari et al. [191] present empirical third-order polynomials with zero intercept as fitting functions with ageing time t, charge and discharge I and SOC as inputs. They fit the model parameters at BOL and after every 3 months for 1 year. Neither temperature information, nor any distributional information is input of their model (Key criterion 1b & 1c).

Thomas et al. [192] propose an empirical rate-based degradation model considering the dependence of T on the SOH_{R}. Compared to other empirical degradation models, their model accumulates the

degradation caused by exposure of the battery to different T for an interval length Δt. Information on I and SOC is not used by the model.

In later work, Thomas et al. [193] apply the method from their previous work to a different data set. Further, in their new work they also output SOH_C^{-1}. Still, there is a lack of information on I and SOC. Also, the model's transferability has not yet been examined (Key criterion 2).

Bamati et al. [194] use the $SOH(t_1)$, as well as averages of temperature T, current I, voltage V, and discharge cycle time t_{disch}. They apply these features to a nonlinear autoregressive with external input (NARX) RNN. For multi-step predictions they use the predicted output of the RNN as input for the next cycle-step. As the authors note, this leads to accumulation of the prediction error. Still, they obtain a RMSE of 3 % on the NASA data set [128] for 30-cycle-ahead prediction and <2 % on an Oxford dataset [195].

Chiodo et al. [196] apply the model proposed in [197] and solve its partial differential equations analytically. They represent the battery operation by the expected charge current λ_{ch} and the expected current variation frequency ψ in events/ minutes. Also, an expected value of the discharge current λ_{disch} can be set as an additional input of the method. The current profile is modeled by a Monte Carlo Poisson process. The CC of small subintervals is drawn from an exponential distribution with the constant rate ψ. λ and ψ can either be estimated from historical data or expressed via hypothesis in a scenario. Still, only two input variables λ and ψ, or three input variables when including λ_{disch}, aggregate the current profile. No information about SOC and temperature is input to the method. The method reaches an adjusted determination coefficient (ADC) up to 99.85%.

Jones et al. [108] present an ensemble of 10 eXtreme Gradient Boosting (XGBoost) models with the impedance spectrum $\boldsymbol{s}_k$ before the cycle k as current state information obtained by electrochemical impedance spectroscopy (EIS) and the future load during cycle k as inputs. The model learns the capacity C after the cycle k. For multi-step-ahead predictions the load during the future cycle can be extended to multiple future cycles. The future load is specified as concatenation of the charge and discharge currents. Thus, for the used dataset with two CC steps limited to 15 min length, the future load vector is still quite short even for long forecast horizons. However, this changes for more variable data from discharging in vehicle operation. Also, no information on temperature and SOC is considered. The mean error is 8.2 % over all forecast horizons. Both current state information and future load are necessary for a good forecast. Only using the state information or the future load results in 20.7 % and 15.4 % error respectively. Increasing the forecasting horizon decreases the model fit down to still $R^2 = 0.75$ for forecasting 40 cycles into the future.

Lopez-Vilanuvea et al. [198] describe an empirical calendar ageing model with discretized subintervals when SOC and temperature T change. All subintervals represented by their individual duration and a factor depending on SOC and T are then summed to obtain the global capacity loss ΔC. Given the fact that parking periods are long in BEV operation applying an empirical model with discretized subintervals is easier for parking than for charging or discharging operation. Also, the SOC will likely be constant for parking. Only the temperature T may vary during day and night.

Lu et al. [199] describe the future operation conditions of the battery as vectors each for the discharge and charge current with their elements corresponding to a single future cycle. Together with capacity-voltage data from early cycling these vectors are input of a gated recurrent unit (GRU) that learns the charge and discharge capacity degradation. Similar to Lopez-Vilanuvea et al. [198], path dependence is considered by the sequence input, but further discretization on sub-cycle-level, e.g. relevant for discharge operation of BEVs is not addressed. The model achieves a median prediction RMSE of 2.4 % and 2.3 % for NMC and LFP batteries respectively.

Sui et al. [200] present a hybrid method based on five physical empirical models. These consider $\bar{T}$, $\overline{SOC}$, $\bar{I}$, overall time t, and rest time factor F_{Rest}. Based on their output, a physical-informed LSTM outputs the corresponding past capacity fade. The past capacity fade is input of a second LSTM model that outputs the future capacity fade. In that sense, the second LSTM model is only autoregressive, but the concrete operational conditions are given to it implicitly via the physical-informed LSTM. Still the

operational conditions cannot be varied for different cycles given the method's architecture. The $\overline{MAPE}$ of three test batteries is 10.15 % after 50 % of the battery's life.

Wang et al. [201] apply a sequence-to-sequence (seq2seq) temporal convolutional network (TCN) with encoder-decoder structure. Based on the sequences of past battery operation, past capacity, and the future battery operation the future capacity is learnt. For this method battery operation is described by rest time t_{rest}, current I, temperature T, and cutoff voltage V_{cutoff} which determines the SOC range. The authors also evaluate memory size and percentage utilization of both CPU and GPU which are only rarely given in papers. The proposed TCN has a MAE of 0.0295 Ah over all datasets.

Xu et al. [202] focus on RUL prediction with explicit consideration of varying ambient temperature. They propose a Wiener process and a two-step unbiased estimation method built on maximum likelihood estimation (MLE) with genetic algorithm (GA). The method is more accurate and less uncertain with explicit consideration of varying ambient temperature than without: It reaches an RMSE of 56.4 cycles compared to 139.2 cycles and 127.8 cycles for the Bayesian method and the particle filter-based method respectively. However, they only use a single battery cell with a different ambient temperature every 10 cycles, so the ambient temperature is not variable within a single cycle.[13]

Similar to Xu et al. [202], Kong et al. [107] not only consider varying temperatures in a Wiener process, but they also can input different discharge rates. The battery data used either varies regarding discharge c-rate or regarding a constant ambient temperature. So no changing temperatures as in Xu et al. [202] where considered. The same applies to combinations of changing c-rates and temperatures.

4.2.2 Models with distributional information about future load

Models with distributional information about the future load can either include rainflow counting or only histograms (Section 4.2.2.1 or 4.2.2.2 respectively). Models with rainflow counting may also contain inputs structured as histograms. Histograms in the context of battery ageing are also referred to as load collectives. Wenzl et al. [94] point out that histograms enable easy analysis of how changes in the operational conditions of a battery affect the ageing by adapted, synthetic histograms. This corresponds to the first problem motivating key criterion 1b in Section 2.2.

4.2.2.1 Models with information about future load based on rainflow counting

Rainflow counting is known from damage evaluation of metals and mechanical fatigue analysis [203]. But it can also be used for SOC cycle counting, i.e. to count how often the SOC jumps from one level range to another [204]. For example, SOC changes from the range of 0–10 % SOC to 10–20 % SOC could be counted. A figurative description is to image rain drops flowing and falling down a pagoda roof. Rainflows starting from a lower level interrupt rainflows from higher levels. Rainflow counting enables the consideration of micro-cycles which has been mentioned in Table 3 as a difference of laboratory and real-world battery operation.

Nuhic et al. [71] output the future $C(t_2)$ based on the current $C(t_1)$, rainflow counting of SOC as well as different load collectives. The load collectives are 2D-histograms of I & T and SOC & T. Nuhic et al. [71] use data of six batteries operated in laboratory with real-world driving profiles at different T, C-rates, SOCs, and DODs. Their method learns the degradation behavior of the batteries, but transferability is not given because SVR was used.

Based on their previous work [71], Nuhic et al. [205] introduce an improvement by adding and combining input information regarding the ΔSOC, $\emptyset SOC$, charging & discharging C-rate, and Q_{thrpt}. In this work for simplicity they only consider $\Delta SOC > 2$ % with the rainflow counting method, but smaller ΔSOC are considerable for recuperation of BEVs. Nuhic et al. [205] also identify that a simplification of the current is necessary to prevent a large amount of data. They propose the calculation of a constant, mean C-rate for discharging and charging for each cycle determined with the rainflow counting method. After estimating the four parameters of the defined model equation, a maximum error bound of 5 % is reached. For a modified current profile, the error bound increases to a maximum of 8 %. Nuhic et al. [205] note that their work is limited to cyclic ageing only, but calendar ageing should

[13] The authors only describe the battery cell is from the CALCE dataset, but it seems that they used cell CX2-4.

be considered in future work. In contrast to most other work found, Nuhic et al. [205] use a SOC profile inspired by real-life current profiles in a one year laboratory test.

Building on their previous work in [71,205], Nuhic et al. [96] add "nested" load collectives. These include nested histograms for SOC, T_{mean}, V_{mean}, and C-rate based on separate SOC cycles determined by the rainflow counting known from Nuhic et al. [71]. E.g. a nested histogram is structured as follows: First, the cycle's T_{mean} is binned, e.g. from 20 °C to 30 °C. Second, within this bin the cycle's V_{mean} is differentiated into further bins, e.g. from 3.8 V to 4.1 V. Finally, within this bin a 2D histogram with bins of c-rate and SOC is created. So overall a 4D histogram is created. The histograms in their previous work [205] are based on separate SOC cycles determined by the rainflow counting. This means only the time window of a certain SOC cycle is considered for counting in the histograms. This is in contrast to Richardson et al. [185] and von Bülow et al. [88], who use the time window of the complete time horizon at once for their histograms. A further difference is that Nuhic et al. [96] count the amount of SOC cycles having values like T_{mean} in a certain range, but the histograms of Nuhic et al. [71], Richardson et al. [185], and von Bülow et al. [88] count the time spend in an operational state. When considering rainflow counting separately from the histograms like in [71], information on the SOC or voltage level of the (micro-)cycles is lost. This is solved in the last work of Nuhic et al. [96] by using nested histograms which connect the rainflow counting with voltage level information.

Stroe [206] proposes a model in his PhD thesis that is based on rainflow-cycle counting. All identified cycles are summarized in a histogram by their cycle depth and $\overline{SOC}$ as well as a separate T profile and rest time t_{rest}. Precise information on I and T is not input of the model so important stressors in real-world operation are missing (Key criterion 1c).

4.2.2.2 Models with information about future load only based on histograms

Richardson et al. [185] present a GPR model with current $C(t_1)$, total time elapsed during the load $\Delta t = t_2 - t_1$, the charge throughput $Q_{\mathrm{thrpt,charge}}$, the absolute time elapsed since BOL t_1, and lastly histogram-like features. These histogram-like features are the time elapsed during which certain conditions regarding intervals of T and I are met. E.g. one input is the time elapsed during 2 A to 3 A. The model's output is ΔC one cycle later so consequently the histograms are also created only for a single cycle. However, the bins of the model's inputs are very broad and do not consider charging information separate from discharging. Thus, the model requires adaption before being able to capture the variability of real-world data (Key criterion 1c).

Von Bülow et al. [88] train MLP models with $SOH(t_1)$ and combined histograms of T, SOC & I as inputs. They forecast the ΔSOH over several cycles based on histograms of the operational data of these cycles. The histograms from Richardson et al. [185] are one dimensional (1D) histograms, e.g. a bin is $2A < I < 3A$. Von Bülow et al. [88] extend these 1D histograms to 2D and 3D histograms which combine bins of two or three signals respectively. For example, a bin is $0C < I < 3C$ and $28\ °C < T < 31\ °C$. The examined 2D histograms are T & SOC, I & SOC, and I & T (Variant A) and T & SOC, I & SOC (Variant B, like variant A without I & T). The 3D histogram has T & I & SOC. They examine different sampling granularities of the histograms and find that 2D histograms work sufficiently well compared to 3D histograms.

Nuhic et al. [71] also propose two parameter instantaneous value (dwell time-) counting which is equivalent to the 2D histogram-like features of von Bülow et al. [88]. Nuhic et al. [71] combine I & T as well as SOC & T.

Frisk et al. [207] apply Random Survival Forests (RSF) to estimate the RUL of lead-acid batteries. They express the RUL as function $\mathcal{B}(t; t_0, \mathcal{V})$ which describes the probability that the battery of a specific vehicle $\mathcal{V}$ will last at least t time units after t_0. They use data from 33,603 Scania heavy-duty trucks from 5 European markets with 291 variables including 17 histograms. Of these they select the 30 most important variables using an AUC-based score. These include among others: the total distance driven, the truck's time of delivery, the number of days in use and histogram values like the time spend at low battery voltage at relatively low temperatures of –5 to 10 °C, at low battery voltage in general, as well as low (<20 %) and high (>80 %) SOC without battery load. They point out that it is not sufficient to

build a RUL prediction model only on calendar time and mileage. The authors do not provide a performance metric of their final model.

Zhang et al. [208] examine SVR, RFR, GPR, and ANN with statistical properties of histograms as features. The statistical properties of the histograms are: Maximum, minimum, range, average, variance, skewness, kurtosis, 5th moment, and 6th moment. Spearman correlation analysis is used to identify the relevant statistical properties that serve as model inputs. The histograms are of T, charging and discharging I, charging and discharging V, and total Q_{thrpt}. They use three public datasets [77,126,127] and a non-public real-world vehicle dataset. For the vehicle dataset additionally the SOC is differentiated in separate histograms for charging, driving, and parking mode, T is differentiated for parking and driving mode, and DOD is added. However, the statistical properties of the V-histogram are not used. As further adaption, the accumulated parking time and total time duration are added. RFR outperforms SVR, GPR, and ANN on all datasets. Its maximum MAPE is 4.21 % on the NASA dataset, and 1.41 % on the real-world vehicle dataset. Model transfer from one dataset to another has not been examined yet (Key criterion 2). A challenge will be that the most correlating features are not the same for the different datasets.

Greenbank and Howey [52] generate histograms of V, T, I, absolute current $|I|$, power P, and absolute power $|P|$. They determine the size of the bins from the 1st, 33rd, 67th, and 99th percentiles of these histograms and derive their features from these percentiles. Disadvantageously, this can only be done after all signal values have been recorded. So, the advantage of time series aggregation in histograms regarding data saving and transfer is lost. Compared to other histogram-based features like in [88], Greenbank and Howey [52] have overlapping bins: For example, the second voltage bin is from 2 V to 3.51 V, which is simply the sum of the first bin from 2 V to 3.12 V and the forth bin from 3.12 V to 3.51 V. Overall, they generate 74 feature which they reduce to 5 features using Pearson's correlation coefficient. As inputs of a GPR these features reach a mean RMSE of 0.17 %. The same work appears also in the PhD thesis of Greenbank [209].

Table 6: Summary of SOH forecasting models. Symbols are defined in Table 5. “x” means yes. “-“ means no.

Ref.	Citations on Google Scholar[14]	Model type[15]	Public data set[16]	Model inputs (See symbols in Table 5)	Key criterion					Open source		Model performance[17]	Overfitting checked	Output value	Forecast horizon
					1a	1b	1c	2	3						
					Info about future load	Aggregated info about future load	Suitable for real-world operation	Transfer	2nd life applicability	Data	Code				
SOH forecasting models without information about future load (Section 4.1)															
[91]	359	GPR	[128]	k	-	-	-	-	x	x	-	$RMSE = 0.08$[18]	-	SOH	-
[175]	102	Empirical	- & [128]	k	-	-	-	-	x	-/x	-	$RMSE = 2.5\ \%$	x	SOH	-
[176]	19	Linear	-	k	-	-	-	-	x	-	-	$MSE = 1.7$	-	SOH	-
[177]	119	Bayesian	-	k	-	-	-	-	x	-	-	$MAD = 0.02$	-	ΔC	1 cycle
[210]	0	LR, RFR, RNN, LSTM	-	t in d	-	-	-	x	x	-	-	$MSE = 3.02$	-	$SOH(t_2)$	100-400 d

[14] Accessed 21.10.2022.

[15] Acronyms of model types: Gaussian process regression (GPR), linear regression (LR), random forest regression (RFR), recurrent neural network (RNN), long short-term memory (LSTM), multiple layer perceptron (MLP), convolutional neural net (CNN), nonlinear autoregressive dynamic network with external inputs (NARX), support-vector regression (SVR), stacked long short-term memory (SLSTM), least-angle regression (LARS), last absolute shrinkage and selection operator (lasso), similarity–based modeling (SBM), Multivariable Fractional Polynomial (MFP), Bayesian Neural Network (BNN), Random Survival Forests (RSF), variational MLP (vMLP), gated recurrent unit (GRU), temporal convolutional network (TCN).

[16] “-“ means own, non-public data set.

[17] Acronyms of metrics: Root mean squared error (RMSE), mean squared error (MSE), mean absolute deviation (MAD), mean average error (MAE), mean average percentage error (MAPE), absolute error (AE), adjusted determination coefficient (ADC).

[18] For prediction horizon > 20 cycles

Ref.	Citations on Google Scholar[14]	Model type[15]	Public data set[16]	Model inputs (See symbols in Table 5)	Key criterion					Open source		Model performance[17]	Overfitting checked	Output value	Forecast horizon
					1a	1b	1c	2	3						
					Info about future load	Aggregated info about future load	Suitable for real-world operation	Transfer	2nd life applicability	Data	Code				
[211]	14	two variational MLPs	[126,128]	$Q_{\text{thrpt,discharged}}$	-	x	-	-	x	x	-	Not given	-	C and R_i	-
[86]	16	Empirical	[128]	k, accumulated t_rest, k after a regeneration due to rest time	-	x	-	-	x	x	-	$RMSE = 0.0189$	-	$C(t)$	-
[212]	66	Dilated CNN	[127]	V_terminal, I, T_cell of last four cycles	-	-	-/x	-	-	x	-	$MAPE = 10.6\ \%$	x	RUL	-
[127]	790	Elastic net	[127]	features derived from the first 100 discharge voltage curves	-	-	-	-	-	x	x	$RMSE = 51\ cycles$	x	cycle life	-
[105]	46	LSTM	[129]	$C(t)$ up to present	autoregressive			-	x	x	x	$MAPE = 1.1\ \%$	x	$C(t)$	-
[168]	0	RNN	[127,129]	$C(t)$ & $R_\text{i}(t)$ up to present	autoregressive			-	x	x	x	$MAPE =$ 2.37 % & 1.24 %	x	$C(t)$ & $R_\text{i}(t)$	-
[178]	10	Among others: CNN	[127]	features derived from the first 100 discharge voltage curves	-	-	-	-	-	x	x	$RMSE = 17$ cycles	x	cycle life	-
[179]	0	VMLP	[126]	E	-	-	-	-	x	x	-	Not given	-	C	-

Ref.	Citations on Google Scholar[14]	Model type[15]	Public data set[16]	Model inputs (See symbols in Table 5)	Key criterion					Open source		Model performance[17]	Overfitting checked	Output value	Forecast horizon
					1a	1b	1c	2	3						
					Info about future load	Aggregated info about future load	Suitable for real-world operation	Transfer	2nd life applicability	Data	Code				
SOH forecasting models without distributional information about future load (Section 4.2.1)															
[181]	33	GPR	-	Δt, T^{-1}, SOC	x	x	-	-	x	-	-	$MAE = 0.31$ %	x	ΔC	30-60 d
[182]	45	GPR	-	Q_{thrpt}, T^{-1}, DOD, $\emptyset SOC$, charging & discharging C-rate	x	x	-	-	x	-	-	$MAE = 0.58$ %	x	ΔC	4-12 kAh
[183]	5	GPR	-	Join [181,182]	x	x	-	-	x	-	-	$MAE = 0.78$ %	-	ΔC	17-21 d & 29.9-84.4 Ah
[153]	26	Semi-empirical	-	k, T_{ambient}, C-rate, T_{rest}, SOC_{rest} , t_{rest}	x	x	-	-	x	-	x	$RMSE = 0.9916$	-	ΔC	-
[153]	26	GPR	-	T_{surface}, charging & discharging C-rate, k, T_{rest}, SOC_{rest}, t_{rest}	x	x	-	-	x	-	x	$RMSE = 0.0458$	-	$C(t_2)$	-
[153]	26	NARX	-	Same as GPR in [153]	x	x	-	-	x	-	x	$RMSE = 0.0099$	x	$C(t_2)$	-
[184]	391	SVR	-	$SOH(t_1)$, T_{min}, T_{max}, Δt, I_{mean}, Q_{thrpt}, SOC_{max}, ΔSOC	x	x	-	-	x	-	-	$MAPE_{\text{max}} = 20$ %	x	$SOH(t_2)$	1 cycle

Ref.	Citations on Google Scholar[14]	Model type[15]	Public data set[16]	Model inputs (See symbols in Table 5)	Key criterion					Open source		Model performance[17]	Overfitting checked	Output value	Forecast horizon
					1a	1b	1c	2	3						
					Info about future load	Aggregated info about future load	Suitable for real-world operation	Transfer	2nd life applicability	Data	Code				
[213]	9	SLSTM	[127]	k, $\emptyset T$, R_{i}	x	x	-	-	x	x	-	$RMSE = 0.0019$	-	$C(t_2)$	30 % of cycle life
[161]	83	LARS, Ridge, Lasso, Elastic Net	-	Output energy, I sign alternation, distance, T_{rest}, $t_{\mathrm{experimental}}$ in d	x	x	-	-	x	-	-	$AE_{\max} = 0.46$	x	$C(t_2)$	2-3 capacity measurements
[214]	6	SBM	[215]	k, $I_{\mathrm{discharge}}$, ΔSOC, $\emptyset$ SOC-SR[19]	x	x	-	-	x	x	-	Not given	-	$\frac{dC(t_2)}{dk}$	1 cycle
[120]	173	GPR	-	$C(t-i), \dots, C(t)$ with $i = 0, \dots, 4$, T_{ambient}, DOD	x	x	-	-	x	-	-	$RMSE = 0.09$	x	$C(t_2)$	1 cycle
[89]	5	BNN	-	C-rate, SOC, T, t	x	x	-	-	x	-	-	$MAE \cong 0.5$ %	-	ΔC	-
[186]	13	LSTM	-	$C(t)$, Δt, SOC_{storage}, T_{storage}	x	-	-	x	x	-	-	$RMSE = 0.0008$	x	$C(t + \Delta t)$	$\Delta t = 720h$
[187]	57	-	-	Count events: 1) high I_{charge}, 2) high I_{charge} & low	x	-/x	-	-	-	-	-	Not given	-	-	-

[19] The SOC-SR (SOC swing range) is the range in which SOC-S varies.

Ref.	Citations on Google Scholar[14]	Model type[15]	Public data set[16]	Model inputs (See symbols in Table 5)	Key criterion					Open source		Model performance[17]	Overfitting checked	Output value	Forecast horizon
					1a	1b	1c	2	3						
					Info about future load	Aggregated info about future load	Suitable for real-world operation	Transfer	2nd life applicability	Data	Code				
				T, 3) high I_{charge} & high DOD											
[188]	2	MFP	[126]	$C(k)$, from discharging: $\overline{T_{\text{min}}}$, $\overline{T_{\text{max}}}$, $\bar{I}$, Δt, λ_{short}, Δt_{rest}, $\overline{V_0}$, $\overline{\Delta V}$, $\overline{C_{\text{approx}}}$	x	x	-	-	x	x	-	$RMSE_{\text{max}} = 0.1383$[20]	x	$\Delta C(k+m)$	Approx. m=50 cycles
[189]	13	GPR, SVM, LR	-	k, charge & discharge I & T, T_{storage}, SOC_{storage}	x	-	-	-	x	-	-	$RMSE = 0.2956$	x	$C(k)$	-
[190]	5	Empirical	-	$C(t)$, charge & discharge I, T, DOD	x	-	-	-	x	-	-	Not given	x	ΔC	1 s
[191]	130	Empirical	-	t, charge & discharge I & SOC	x	-	-	-	x	-	-	$AE = 0.02$[21]	-	ΔSOH	-
[170]	13	GPR	-	R_i, $\frac{\partial R_i}{\partial t}$, calendar age, Q_{thrpt}, k,	x	x	-	-	-	-	-	Balanced accuracy = 73 %[22]	x	RUL_{R}	0-8 weeks

[20] Best feature set (MFPc) and worst battery (RW12) results in maximum RMSE.
[21] Only graphical and qualitative results, except of this error for profiles at $SOC = 40$ % after 1 year.
[22] At a prediction horizon of 8 weeks until EOL.

Ref.	Citations on Google Scholar[14]	Model type[15]	Public data set[16]	Model inputs (See symbols in Table 5)	Key criterion					Open source		Model performance[17]	Overfitting checked	Output value	Forecast horizon
					1a	1b	1c	2	3						
					Info about future load	Aggregated info about future load	Suitable for real-world operation	Transfer	2nd life applicability	Data	Code				
				cumulative time spent at float charge, $\bar{T}$, and $\bar{V}$											until EOL
[192]	60	Empirical	-	$(T, \Delta t)_i$, $SOH_{\mathrm{R}}(t_1)$	x	-	-	-	x	-	-	$\sigma_\varepsilon = 0.01$	-	SOH_{R}	$\Delta t = 1h$
[193]	5	Empirical	-	$(T, \Delta t)_i$, $SOH(t_1)$	x	-	-	-	x	-	-	$\sigma_{\varepsilon,R} = 0.01$, $\sigma_{\varepsilon,C} = 0.002$	-	SOH_{R}, SOH_{C}^{-1}	$\Delta t = 1h$
[194]	2	NARX-RNN	[128,195]	$SOH(t_1)$, I_{mean}, T_{mean}, V_{mean}, $t_{\mathrm{dis,mean}}$	x	x	-	-	x	x	-	$RMSE \leq 3$ %	-	SOH	1 or 30 cycles
[196]	0	Empirical	-	λ_{ch}, λ_{disch}, ψ	x	x	-	-	x	-	-	$ADC \leq 99.85$ %	-	C	-
[108]	1	XGBoost	[216]	impedance spectrum $\boldsymbol{s}_k$, I_{k+j}	x	-	-	-	x	x	x	$\overline{Error} = 8.2$ %	x	C_{k+j}	1-40 cycles
[198]	0	Empirical	-	Vectors of SOC & T	x	-	-	-	x	-	-	Not given	-	ΔC	-
[199]	4	GRU	[77,127,217]	Vectors of I_{ch} & I_{disch}	x	-	-	-	x	x	-	$\overline{RMSE} = 2.3$ %	-	C	-
[200]	0	Hybrid	[128]	$\bar{T}$, $\overline{SOC}$, $\bar{I}$, t, F_{Rest}	x	x	-	-	-	x	-	$\overline{MAPE} = 10.15$ %	x	RUL	-
[201]	0	TCN	[128,218–220]	t_{rest}, I, T, V_{cutoff}	x	-	-	-	x	x	-	$MAE = 0.0295\ Ah$	x	C	-

Ref.	Citations on Google Scholar[14]	Model type[15]	Public data set[16]	Model inputs (See symbols in Table 5)	Key criterion					Open source		Model performance[17]	Overfitting checked	Output value	Forecast horizon
					1a	1b	1c	2	3						
					Info about future load	Aggregated info about future load	Suitable for real-world operation	Transfer	2nd life applicability	Data	Code				
[202]	41	Wiener Process	[218]	T_{ambient}	x	-	-	-	-	x	-	$RMSE = 56.4$	-	RUL	-
[107]	2	Wiener Process	- & [221]	T_{ambient}, C-rate	x	-	-	-	-	-/x	-	$\overline{Error} = -3.05$	-	RUL	-
SOH forecasting models with information about future load based on rainflow counting (Section 4.2.2.1)															
[71]	516	SVR	-	$C(t_1)$, rainflow counting SOC, load collective I over T and SOC over T	x	x	x	-	x	-	-	$MSE \cong 0.0004$	x	$C(t_2)$	$\cong$ 8-15 d
[205]	1[23]	Equation with four parameters	-	ΔSOC, $\emptyset SOC$, charging & discharging C-rate, Q_{thrpt}	x	x	x	-	x	-	-	$AE_{\max} = 8\ \%$	x	ΔC	$\cong$ 2-5 kAh
[96]	22	SVR	-	"nested" load collective of SOC-classes, T, V, SOC, C-rate	x	x	x	-	x	-	-	Only graphically	-	$C(t_2)$	$\cong$ 50 d

[23] The work of Nuhic et al. [205] is not publicly available. Thus, it is not listed on Google Scholar. On ReserachGate one citation is mentioned. The first author kindly provided the work upon request.

Ref.	Citations on Google Scholar[14]	Model type[15]	Public data set[16]	Model inputs (See symbols in Table 5)	Key criterion					Open source		Model performance[17]	Overfitting checked	Output value	Forecast horizon
					1a	1b	1c	2	3						
					Info about future load	Aggregated info about future load	Suitable for real-world operation	Transfer	2nd life applicability	Data	Code				
[206]	26	Empirical: Power law & linear	-	Histogram by cycle depths & $\overline{SOC}$, profile of T, t_{rest}	x	x	-	-	x	-	-	$MAPE_{\max} = 10.24\ \%$	-	ΔC	1 week
SOH forecasting models with information about future load only based on histograms (Section 4.2.2.2)															
[185]	100	GPR	[128]	$C(t_1)$, Δt, $Q_{\text{thrpt,charge}}$, t_1, T & I histogram-like	x	x	-	-	x	x	-	$RMSE = 0.0201$	x	ΔC	1 cycle
[88]	3	MLP	[127]	$SOH(t_1)$, T, SOC & I histogram-like	x	x	x	x[24]	x	x	-	$RMSE_{\text{test}} = 0.084$[25]	x	ΔSOH	25-530 cycles
[207]	40	RSF	-	5 non-histogram variables, 12 bin variables, 13 derived histogram variables	x	x	x	-	-	-	-	Not given	-	RUL	-
[208]	10	SVR, RFR, GPR, ANN	- & [77,126,127]	Statistical properties of histograms of T, charging and discharging I,	x	x	x	-	x	-/x	-	$MAPE_{\max} = 4.21\ \%$	x	ΔC	1 cycle

[24] In follow-up work: [174].
[25] From Table 12 F-W9-2D, variant A $w_s = 25$.

Ref.	Citations on Google Scholar[14]	Model type[15]	Public data set[16]	Model inputs (See symbols in Table 5)	Key criterion					Open source		Model performance[17]	Overfitting checked	Output value	Forecast horizon
					1a	1b	1c	2	3						
					Info about future load	Aggregated info about future load	Suitable for real-world operation	Transfer	2nd life applicability	Data	Code				
				charging and discharging V, and total Q_{thrpt}											
[52]	18	GPR	[77,127]	Histograms of V, T, I, $\lvert I\rvert$, P, $\lvert P\rvert$	x	x	x	-	x	x	-	$\overline{RMSE} = 0.0017$	x	ΔC	$\Delta t = 12h$

5 Conclusion

In this paper, six key criteria for SOH forecasting models shown in Table 2 were derived from a user's perspective of battery designer and BEV fleet manager. The existing literature of SOH forecasting models was assessed and filtered regarding these key criteria. Then, the remaining literature was hierarchically structured in four groups visualized in Figure 4 regarding the model's input information of the future battery load. Furthermore, we observed no clear differentiation of SOH estimation, prediction, and forecast in the reviewed literature so we provided a differentiation of these terms in Section 2.

This survey gained insights in possible input values of SOH forecasting models. Also, rain flow counting and histograms as time series aggregation methods maintaining distributional information for SOH forecasting models were presented. Only 10 SOH forecasting models use distributional information about the future battery operational load. The majority either cannot input information about the future load or the information is only non-distributional. The latter means that constant load, e.g. regrading ΔSOC, T_{rest}, and SOC_{rest} is assumed for the whole forecasting horizon. This is an unrealistic assumption in real-world operation of BEVs. In existing literature, only machine learning models like SVR, GPR, and MLP were shown to work with distributional information of battery operation. In contrast to humans and other models, machine learning models are able to learn the complex dependencies of battery operation and battery ageing from data.

As pointed out by the Venn diagram Figure 5, the majority of the five chosen key criteria is only satisfied by a few methods. Model transfer has only been examined once, indicating that more research is required on key criterion 2. Key criterion 3 can easily be fulfilled by choosing the SOH as output value. Overall, the use and development of SOH forecasting models applicable in real-world operation according to the defined key criteria are still in an early stage. However, the evaluation of the found methods is only regarding the finite set of the five chosen key criteria in Section 2.2. Other key criteria, e.g. related to the technical implementation of the methods are not considered. One could consider the necessary amount of training data, required computational resources for training and interference, and size of the model (in storage MB or number of parameters). These key criteria are out of scope for this review but will become important once the field of SOH forecasting advances.

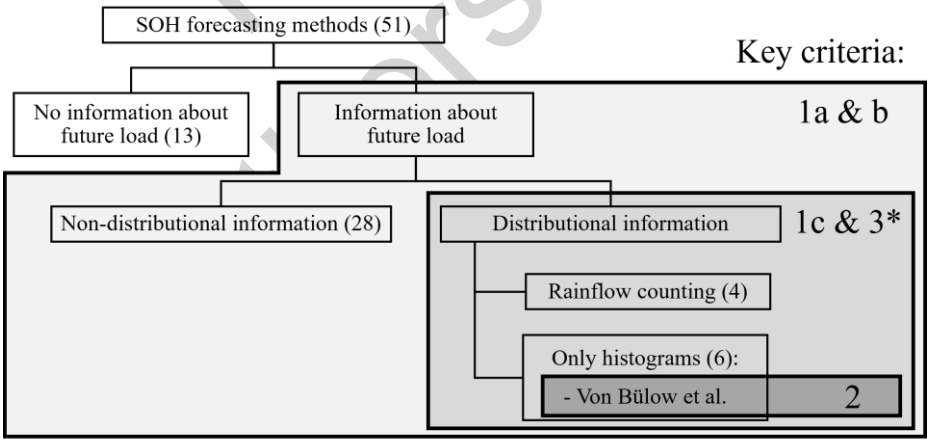

Figure 5: Venn diagram based on method hierarchy regarding input data of the methods (see Figure 4). The fulfilled critical key criteria correspond to the colored areas. The key criteria are defined in Table 2. *Key criteria 1c and 3 are only not fulfilled for [185,206] and [207] respectively.

The comparability of the performance results of the presented models is difficult because of different operational data, different output values, different metrics, and different forecast horizons used. Furthermore, a lack of open-source availability of both code and data complicates comparisons. Currently, no standard data set from real-world operation exists for battery SOH forecasting models like ImageNet, MNIST or CIFAR for image classification models. Such open-source datasets give different researchers the opportunity to compare the performance results, e.g. of their data augmentation

techniques [222]. A publicly available data set not from laboratory battery operation, but from real-world vehicle operation would enable benchmarking of SOH forecasting models applicable in real-world vehicle operation. Thus, it would accelerate progress in the research field.

6 References

[1] Verband der Automobilindustrie e.V. (VDA), First global e-mobility ranking. https://en.vda.de/en/press/press-releases/210423-First-global-e-mobility-ranking.html, 2021 (accessed 7.11.2021).

[2] International Energy Agency (IEA), Global Electric Vehicle Outlook 2022. https://iea.blob.core.windows.net/assets/ad8fb04c-4f75-42fc-973a-6e54c8a4449a/GlobalElectricVehicleOutlook2022.pdf, 2022 (accessed 13.06.2022).

[3] J. Warner, The handbook of lithium-ion battery pack design, Elsevier Science, Amsterdam, 2015.

[4] R. Dorn, R. Schwartz, B. Steurich, Battery management system, in: R. Korthauer (Ed.), Lithium-Ion Batteries: Basics and Applications, Springer Berlin Heidelberg, Berlin, Heidelberg, 2018, pp. 165–175.

[5] W. Waag, D.U. Sauer, SECONDARY BATTERIES – LEAD–ACID SYSTEMS | State-of-Charge/Health, in: J. Garche (Ed.), Encyclopedia of electrochemical power sources, Elsevier, Amsterdam, The Netherlands, 2009, pp. 793–804.

[6] Verband der Elektrotechnik Elektronik Informationstechnik e. V. (VDE), Battery Systems for Multiple Units. https://www.vde.com/resource/blob/2068324/a35ebed9833dae59d8cb1451368203bd/vde-study-battery-systems-data.pdf, 2018 (accessed 20.04.2022).

[7] M. Dubarry, M. Tun, G. Baure, M. Matsuura, R.E. Rocheleau, Battery Durability and Reliability under Electric Utility Grid Operations: Analysis of On-Site Reference Tests, Electronics. 10 (2021). https://doi.org/10.3390/electronics10131593.

[8] L. Yao, S. Xu, A. Tang, F. Zhou, J. Hou, Y. Xiao, Z. Fu, A Review of Lithium-Ion Battery State of Health Estimation and Prediction Methods, WEVJ. 12 (2021) 113. https://doi.org/10.3390/wevj12030113.

[9] H. Tian, P. Qin, K. Li, Z. Zhao, Review and recent advances in battery health monitoring and prognostics technologies for electric vehicle (EV) safety and mobility, Journal of Cleaner Production. 261 (2020). https://doi.org/10.1016/j.jclepro.2020.120813.

[10] S.M. Rezvanizaniani, Z. Liu, Y. Chen, J. Lee, Review and recent advances in battery health monitoring and prognostics technologies for electric vehicle (EV) safety and mobility, J. of Power Sources. 256 (2014) 110–124. https://doi.org/10.1016/j.jpowsour.2014.01.085.

[11] A. Barré, B. Deguilhem, S. Grolleau, M. Gérard, F. Suard, D. Riu, A review on lithium-ion battery ageing mechanisms and estimations for automotive applications, J. of Power Sources. 241 (2013) 680–689. https://doi.org/10.1016/j.jpowsour.2013.05.040.

[12] S. Wang, S. Jin, D. Bai, Y. Fan, H. Shi, C. Fernandez, A critical review of improved deep learning methods for the remaining useful life prediction of lithium-ion batteries, Energy Reports. 7 (2021) 5562–5574. https://doi.org/10.1016/j.egyr.2021.08.182.

[13] L. Wu, X. Fu, Y. Guan, Review of the Remaining Useful Life Prognostics of Vehicle Lithium-Ion Batteries Using Data-Driven Methodologies, Appl. Sciences. 6 (2016) 166. https://doi.org/10.3390/app6060166.

[14] M.S.H. Lipu, M.A. Hannan, A. Hussain, M.M. Hoque, P.J. Ker, M.H.M. Saad, A. Ayob, A review of state of health and remaining useful life estimation methods for lithium-ion battery in electric vehicles, Journal of Cleaner Production. 205 (2018) 115–133. https://doi.org/10.1016/j.jclepro.2018.09.065.

[15] Y. Li, K.L. Liu, A.M. Foley, A. Zulke, M. Berecibar, E. Nanini-Maury, J. van Mierlo, H.E. Hoster, Data-driven health estimation and lifetime prediction of lithium-ion batteries: A review, Renewable and Sustain. Energy Rev. 113 (2019). https://doi.org/10.1016/j.rser.2019.109254.

[16] W. Waag, C. Fleischer, D.U. Sauer, Critical review of the methods for monitoring of lithium-ion batteries in electric and hybrid vehicles, J. of Power Sources. 258 (2014) 321–339. https://doi.org/10.1016/j.jpowsour.2014.02.064.

[17] M. Lucu, E. Martinez-Laserna, I. Gandiaga, H. Camblong, A critical review on self-adaptive Li-ion battery ageing models, J. of Power Sources. 401 (2018) 85–101. https://doi.org/10.1016/j.jpowsour.2018.08.064.

[18] Q. Badey, G. Cherouvrier, Y. Reynier, J.-M. Duffault, S. Franger, Ageing forecast of lithium-ion batteries for electric and hybrid vehicles, Current Topics in Electrochemistry (2011) 65–79. https://doi.org/.

[19] N. Collath, B. Tepe, S. Englberger, A. Jossen, H. Hesse, Aging aware operation of lithium-ion battery energy storage systems, J. of Energy Storage. 55 (2022) 105634. https://doi.org/10.1016/j.est.2022.105634.

[20] B.-A. Enache, G.-C. Seritan, S.-D. Grigorescu, C. Cepisca, F.-C. Adochiei, V.-V. Argatu, T.I. Voicila, A Battery Screening System for Second Life $LiFePO_4$ Batteries, in: 2020 International Conference and Exposition on Electrical And Power Engineering (EPE), IEEE, 2020, pp. 298–301.

[21] Z. Zhou, A. Ran, S. Chen, X. Zhang, G. Wei, B. Li, F. Kang, X. Zhou, H. Sun, A fast screening framework for second-life batteries based on an improved bisecting K-means algorithm combined with fast pulse test, J. of Energy Storage. 31 (2020) 101739. https://doi.org/10.1016/j.est.2020.101739.

[22] Münchener Rückversicherungs-Gesellschaft, Battery performance now insurable – Innovative Munich Re coverage paves the way for renewable energy. https://www.munichre.com/content/dam/munichre/contentlounge/website-pieces/documents/Munich-Re-PM-2019-03-07_en.pdf, 2019 (accessed 23.04.2022).

[23] M.N. Mladenović, Mobility as a Service, in: R. Vickerman (Ed.), International Encyclopedia of Transportation, Elsevier, San Diego, CA, USA, 2021, pp. 12–18.

[24] MOIA GmbH, Zwischenbilanz MOIA Ridepooling in Hamburg (Stand: 30.11.2021). https://www.moia.io/news-center/MOIA_Factsheet_Hamburg_DE.pdf, 2021 (accessed 21.12.2021).

[25] E. Meissner, G. Richter, The challenge to the automotive battery industry, J. of Power Sources. 144 (2005) 438–460. https://doi.org/10.1016/j.jpowsour.2004.10.031.

[26] L. Lu, X. Han, J. Li, J. Hua, M. Ouyang, A review on the key issues for lithium-ion battery management in electric vehicles, J. of Power Sources. 226 (2013) 272–288. https://doi.org/10.1016/j.jpowsour.2012.10.060.

[27] S. Saxena, Y. Xing, M.G. Pecht, PHM of Li-ion Batteries, in: M.G. Pecht, M. Kang (Eds.), Prognostics and Health Management of Electronics, John Wiley and Sons Ltd, Chichester, UK, 2018, pp. 349–375.

[28] L. Chen, Z. Lü, W. Lin, J. Li, H. Pan, A new state-of-health estimation method for lithium-ion batteries through the intrinsic relationship between ohmic internal resistance and capacity, Meausrement. 116 (2018) 586–595. https://doi.org/10.1016/j.measurement.2017.11.016.

[29] X. Hu, F. Feng, K.L. Liu, L. Zhang, J. Xie, B. Liu, State estimation for advanced battery management, Renewable and Sustain. Energy Rev. 114 (2019) 109334. https://doi.org/10.1016/j.rser.2019.109334.

[30] K. Singh, T. Tjahjowidodo, L. Boulon, M. Feroskhan, Framework for measurement of battery state-of-health (resistance) integrating overpotential effects and entropy changes using energy equilibrium, Energy. 239 (2022) 121942. https://doi.org/10.1016/j.energy.2021.121942.

[31] A. Farmann, W. Waag, A. Marongiu, D.U. Sauer, Critical review of on-board capacity estimation techniques for lithium-ion batteries in electric and hybrid electric vehicles, J. of Power Sources. 281 (2015) 114–130. https://doi.org/10.1016/j.jpowsour.2015.01.129.

[32] A. Kohs, Batteriemodell zur Prädiktion des Gesundheitszustands von Lithium-Ionen-Batterien, 1st ed., Springer Fachmedien Wiesbaden, Wiesbaden, 2022.

[33] M.-F. Ng, J. Zhao, Q. Yan, G.J. Conduit, Z.W. Seh, Predicting the state of charge and health of batteries using data-driven machine learning, Nat. Mach. Intell. 2 (2020) 161–170. https://doi.org/10.1038/s42256-020-0156-7.

[34] A. Barai, K. Uddin, M. Dubarry, L. Somerville, A. McGordon, P. Jennings, I. Bloom, A comparison of methodologies for the non-invasive characterisation of commercial Li-ion cells, Progress in Energy and Combustion Science. 72 (2019) 1–31. https://doi.org/10.1016/j.pecs.2019.01.001.

[35] N. Noura, L. Boulon, S. Jemeï, A Review of Battery State of Health Estimation Methods, WEVJ. 11 (2020) 66. https://doi.org/10.3390/wevj11040066.

[36] M. Arrinda, M. Oyarbide, H. Macicior, E. Muxika, H. Popp, M. Jahn, B. Ganev, I. Cendoya, Application Dependent End-of-Life Threshold Definition Methodology for Batteries in Electric Vehicles, Batteries. 7 (2021) 12. https://doi.org/10.3390/batteries7010012.

[37] H. Löbberding, S. Wessel, C. Offermanns, M. Kehrer, J. Rother, H. Heimes, A. Kampker, From Cell to Battery System in BEVs, WEVJ. 11 (2020) 77. https://doi.org/10.3390/wevj11040077.

[38] A. Hauser, R.M. Kuhn, High-voltage battery management systems (BMS) for electric vehicles, in: B. Scrosati, J. Garche, W. Tillmetz (Eds.), Advances in battery technologies for electric vehicles, Woodhead Publishing, Cambridge, UK, 2015, pp. 265–282.

[39] A. Kwade, W. Haselrieder, R. Leithoff, A. Modlinger, F. Dietrich, K. Droeder, Current status and challenges for automotive battery production technologies, Nat. Energy. 3 (2018) 290–300. https://doi.org/10.1038/s41560-018-0130-3.

[40] Volkswagen AG, Key components for a new era – the battery system. https://www.volkswagenag.com/en/news/2019/12/key-components-for-a-new-era--the-battery-system.html, 2019 (accessed 20.04.2022).

[41] A. Kampker, Elektromobilproduktion, Springer Berlin Heidelberg, Berlin, Heidelberg, 2014.

[42] International Organization for Standardization (ISO), Secondary cells and batteries containing alkaline or other non-acid electrolytes – Secondary lithium cells and batteries for use in industrial applications, 62620:2014, 2014.

[43] D.U. Sauer, Einfluss der Batteriestreuung und Lebensdauer auf das Batteriesystemdesign. https://www.researchgate.net/profile/Dirk-Uwe-Sauer/publication/299447031_Einfluss_der_Batteriestreuung_und_Lebensdauer_auf_das_Batteriesystemdesign/links/56f8487008ae7c1fda307474/Einfluss-der-Batteriestreuung-und-Lebensdauer-auf-das-Batteriesystemdesign.pdf, 2015 (accessed 10.06.2022).

[44] S.-L. Jeng, C.M. Tan, P.-C. Chen, Statistical distribution of Lithium-ion batteries useful life and its application for battery pack reliability, J. of Energy Storage. 51 (2022) 104399. https://doi.org/10.1016/j.est.2022.104399.

[45] Y. Hua, A.C. Cordoba-Arenas, N. Warner, G. Rizzoni, A multi time-scale state-of-charge and state-of-health estimation framework using nonlinear predictive filter for lithium-ion battery pack

with passive balance control, J. of Power Sources. 280 (2015) 293–312. https://doi.org/10.1016/j.jpowsour.2015.01.112.

[46] O. Juhlin, Modeling of Battery Degradation in Electrified Vehicles. Master Thesis. Linköpings universitet, Linköping, Sweden, 2016. http://urn.kb.se/resolve?urn=urn:nbn:se:liu:diva-134114 (accessed 3.06.2022).

[47] I. Buchmann, BU-302: Series and Parallel Battery Configurations. https://batteryuniversity.com/article/bu-302-series-and-parallel-battery-configurations, 2021 (accessed 8.06.2022).

[48] C.-Y. Chang, P. Tulpule, G. Rizzoni, W. Zhang, X. Du, A probabilistic approach for prognosis of battery pack aging, J. of Power Sources. 347 (2017) 57–68. https://doi.org/10.1016/j.jpowsour.2017.01.130.

[49] T. Bruen, J. Marco, Modelling and experimental evaluation of parallel connected lithium ion cells for an electric vehicle battery system, J. of Power Sources. 310 (2016) 91–101. https://doi.org/10.1016/j.jpowsour.2016.01.001.

[50] D.H. Jung, D.M. Kim, J. Park, S.-i. Kim, T. Kim, Cycle-life prediction model of lithium iron phosphate-based lithium-ion battery module, Int. J. Energy Res. 45 (2021) 16489–16496. https://doi.org/10.1002/er.6895.

[51] M. Aykol, C.B. Gopal, A. Anapolsky, P.K. Herring, B. van Vlijmen, M.D. Berliner, M.Z. Bazant, R.D. Braatz, W.C. Chueh, B.D. Storey, Perspective-Combining Physics and Machine Learning to Predict Battery Lifetime, J. Electrochem. Soc. 168 (2021) 30525. https://doi.org/10.1149/1945-7111/abec55.

[52] S. Greenbank, D.A. Howey, Automated Feature Extraction and Selection for Data-Driven Models of Rapid Battery Capacity Fade and End of Life, IEEE Trans. Ind. Inf. 18 (2022) 2965–2973. https://doi.org/10.1109/TII.2021.3106593.

[53] K. Liu, Z. Wei, C. Zhang, Y. Shang, R. Teodorescu, Q.-L. Han, Towards Long Lifetime Battery, IEEE-CAA JOURNAL OF AUTOMATICA SINICA. 9 (2022) 1139–1165. https://doi.org/10.1109/JAS.2022.105599.

[54] V. Sulzer, P. Mohtat, A. Aitio, S. Lee, Y.T. Yeh, F. Steinbacher, M.U. Khan, J.W. Lee, J.B. Siegel, A.G. Stefanopoulou, D.A. Howey, The challenge and opportunity of battery lifetime prediction from field data, Joule. 5 (2021) 1934–1955. https://doi.org/10.1016/j.joule.2021.06.005.

[55] H. Meng, Y.-F. Li, A review on prognostics and health management (PHM) methods of lithium-ion batteries, Renewable and Sustain. Energy Rev. 116 (2019). https://doi.org/10.1016/j.rser.2019.109405.

[56] Cambridge University Press, Cambridge Advanced Learner's Dictionary, 3rd ed., Cambridge Unversity Press, Cambridge, UK, 2008.

[57] Cambridge University Press, Cambridge Academic Content Dictionary, 1st ed., Cambridge Unversity Press, Cambridge, UK, 2009.

[58] A.S. Hornby, D. Lea, J. Bradbery, Oxford advanced learner's dictionary of current English, 10th ed., 2020.

[59] D. Lea, Oxford learner's dictionary of academic English, 1st ed., Oxford Univ. Press, Oxford, UK, 2014.

[60] A. Stevenson, The Oxford dictionary of English, 3rd ed., Oxford Univ. Press, Oxford, UK, 2010.

[61] S. O'Shea, Cambridge business english dictionary, Ernst Klett Sprachen GmbH; Cambridge Unversity Press, Stuttgart, Cambrigde, 2011.

[62] F. Petropoulos, D. Apiletti, V. Assimakopoulos, M.Z. Babai, D.K. Barrow, S. Ben Taieb, C. Bergmeir, R.J. Bessa, J. Bijak, J.E. Boylan, J. Browell, C. Carnevale, J.L. Castle, P. Cirillo, M.P. Clements, C. Cordeiro, F.L. Cyrino Oliveira, S. de Baets, A. Dokumentov, J. Ellison, P. Fiszeder, P.H. Franses, D.T. Frazier, M. Gilliland, M.S. Gönül, P. Goodwin, L. Grossi, Y. Grushka-Cockayne, M. Guidolin, M. Guidolin, U. Gunter, X. Guo, R. Guseo, N. Harvey, D.F. Hendry, R. Hollyman, T. Januschowski, J. Jeon, V.R.R. Jose, Y. Kang, A.B. Koehler, S. Kolassa, N. Kourentzes, S. Leva, F. Li, K. Litsiou, S. Makridakis, G.M. Martin, A.B. Martinez, S. Meeran, T. Modis, K. Nikolopoulos, D. Önkal, A. Paccagnini, A. Panagiotelis, I. Panapakidis, J.M. Pavía, M. Pedio, D.J. Pedregal, P. Pinson, P. Ramos, D.E. Rapach, J.J. Reade, B. Rostami-Tabar, M. Rubaszek, G. Sermpinis, H.L. Shang, E. Spiliotis, A.A. Syntetos, P.D. Talagala, T.S. Talagala, L. Tashman, D. Thomakos, T. Thorarinsdottir, E. Todini, J.R. Trapero Arenas, X. Wang, R.L.

Winkler, A. Yusupova, F. Ziel, Forecasting, International Journal of Forecasting. 38 (2022) 705–871. https://doi.org/10.1016/j.ijforecast.2021.11.001.

[63] V. Chugh, Estimation, Prediction and Forecasting. https://towardsdatascience.com/estimation-prediction-and-forecasting-40c56a5be0c9, 2020 (accessed 8.12.2021).

[64] M. Döring, Prediction vs Forecasting. https://www.datascienceblog.net/post/machine-learning/forecasting_vs_prediction, 2018 (accessed 8.12.2021).

[65] Z. Guo, X. Qiu, G. Hou, B.Y. Liaw, C. Zhang, State of health estimation for lithium ion batteries based on charging curves, J. of Power Sources. 249 (2014) 457–462. https://doi.org/10.1016/j.jpowsour.2013.10.114.

[66] Y. Fan, F. Xiao, C. Li, G. Yang, X. Tang, A novel deep learning framework for state of health estimation of lithium-ion battery, J. of Energy Storage. 32 (2020) 101741. https://doi.org/10.1016/j.est.2020.101741.

[67] J. Yu, B. Mo, D. Tang, J. Yang, J. Wan, J. Liu, Indirect state-of-health estimation for lithium-ion batteries under randomized use, Energies. 10 (2017) 2012. https://doi.org/10.3390/en10122012.

[68] J. Wu, Y. Wang, X. Zhang, Z. Chen, A novel state of health estimation method of li-ion battery using group method of data handling, J. of Power Sources. 327 (2016) 457–464. https://doi.org/10.1016/j.jpowsour.2016.07.065.

[69] L. Song, K. Zhang, T. Liang, X. Han, Y. Zhang, Intelligent state of health estimation for lithium-ion battery pack based on big data analysis, J. of Energy Storage. 32 (2020) 101836. https://doi.org/10.1016/j.est.2020.101836.

[70] D. Yang, X. Zhang, R. Pan, Y. Wang, Z. Chen, A novel Gaussian process regression model for state-of-health estimation of lithium-ion battery using charging curve, J. of Power Sources. 384 (2018) 387–395. https://doi.org/10.1016/j.jpowsour.2018.03.015.

[71] A. Nuhic, T. Terzimehic, T. Soczka-Guth, M. Buchholz, K. Dietmayer, Health diagnosis and remaining useful life prognostics of lithium-ion batteries using data-driven methods, J. of Power Sources. 239 (2013) 680–688. https://doi.org/10.1016/j.jpowsour.2012.11.146.

[72] D. Cheng, W. Sha, L. Wang, S. Tang, A. Ma, Y. Chen, H. Wang, P. Lou, S. Lu, Y.-C. Cao, Solid-State Lithium Battery Cycle Life Prediction Using Machine Learning, Appl. Sciences. 11 (2021) 4671. https://doi.org/10.3390/app11104671.

[73] D.U. Sauer, H. Wenzl, BATTERIES | Lifetime Prediction, in: J. Garche (Ed.), Encyclopedia of electrochemical power sources, Elsevier, Amsterdam, The Netherlands, 2009, pp. 522–538.

[74] M.A. Ortega - Vazquez, Optimal scheduling of electric vehicle charging and vehicle - to - grid services at household level including battery degradation and price uncertainty, IET gener. transm. distrib. 8 (2014) 1007–1016. https://doi.org/10.1049/iet-gtd.2013.0624.

[75] J. Zhu, I. Mathews, D. Ren, W. Li, D. Cogswell, B. Xing, T. Sedlatschek, S.N.R. Kantareddy, M. Yi, T. Gao, Y. Xia, Q. Zhou, T. Wierzbicki, M.Z. Bazant, End-of-life or second-life options for retired electric vehicle batteries, Cell Reports Physical Science. 2 (2021) 100537. https://doi.org/10.1016/j.xcrp.2021.100537.

[76] E. Martinez-Laserna, E. Sarasketa-Zabala, I. Villarreal Sarria, D.-I. Stroe, M.J. Swierczynski, A. Warnecke, J.-M. Timmermans, S. Goutam, N. Omar, P. Rodriguez, Technical Viability of Battery Second Life, IEEE Trans. on Ind. Applicat. 54 (2018) 2703–2713. https://doi.org/10.1109/TIA.2018.2801262.

[77] P.M. Attia, A. Grover, N. Jin, K.A. Severson, T.M. Markov, Y.-H. Liao, M.H. Chen, B. Cheong, N. Perkins, Z. Yang, P.K. Herring, M. Aykol, S.J. Harris, R.D. Braatz, S. Ermon, W.C. Chueh, Closed-loop optimization of fast-charging protocols for batteries with machine learning, Nature. 578 (2020) 397–402. https://doi.org/10.1038/s41586-020-1994-5.

[78] F. Wankmüller, P.R. Thimmapuram, K.G. Gallagher, A. Botterud, Impact of battery degradation on energy arbitrage revenue of grid-level energy storage, J. of Energy Storage. 10 (2017) 56–66. https://doi.org/10.1016/j.est.2016.12.004.

[79] M. Ecker, J.B. Gerschler, J. Vogel, S. Kaebitz, F. Hust, P.A. Dechent, D.U. Sauer, Development of a lifetime prediction model for lithium-ion batteries based on extended accelerated aging test data, J. of Power Sources. 215 (2012) 248–257. https://doi.org/10.1016/j.jpowsour.2012.05.012.

[80] H. Wenzl, I. Baring-Gould, R. Kaiser, B.Y. Liaw, P. Lundsager, J. Manwell, A. Ruddell, V. Svoboda, Life prediction of batteries for selecting the technically most suitable and cost effective battery, J. of Power Sources. 144 (2005) 373–384. https://doi.org/10.1016/j.jpowsour.2004.11.045.

[81] A.K.S. Jardine, D. Lin, D. Banjevic, A review on machinery diagnostics and prognostics implementing condition-based maintenance, Mech. Syst. and Signal Process. 20 (2006) 1483–1510. https://doi.org/10.1016/j.ymssp.2005.09.012.

[82] J. Zhang, J. Lee, A review on prognostics and health monitoring of Li-ion battery, J. of Power Sources. 196 (2011) 6007–6014. https://doi.org/10.1016/j.jpowsour.2011.03.101.

[83] P. Gasper, K. Smith, Predictive Battery Lifetime Modeling at the National Renewable Energy Laboratory. https://www.osti.gov/biblio/1838001, 2021 (accessed 23.05.2022).

[84] X. Hu, Le Xu, X. Lin, M.G. Pecht, Battery Lifetime Prognostics, Joule. 4 (2020) 310–346. https://doi.org/10.1016/j.joule.2019.11.018.

[85] Y.-H. Lui, M. Li, A. Downey, S. Shen, V.P. Nemani, H. Ye, C. van Elzen, G. Jain, S. Hu, S. Laflamme, C. Hu, Physics-based prognostics of implantable-grade lithium-ion battery for remaining useful life prediction, J. of Power Sources. 485 (2021). https://doi.org/10.1016/j.jpowsour.2020.229327.

[86] L. Deng, W. Shen, H. Wang, S. Wang, A rest-time-based prognostic model for remaining useful life prediction of lithium-ion battery, Neural Computing & Applications. 33 (2021) 2035–2046. https://doi.org/10.1007/s00521-020-05105-0.

[87] Autovista Group Limited, TWAICE Technologies GmbH, TÜV RheinlandMobility, The Power of Signalling. https://twaice.com/wp-content/uploads/2020/06/202006_Battery_Health_Report_TWAICE_Autovista_TÜV-1.pdf, 2020 (accessed 2.12.2021).

[88] F. von Bülow, J. Mentz, T. Meisen, State of health forecasting of Lithium-ion batteries applicable in real-world operational conditions, J. of Energy Storage. 44 (2021) 103439. https://doi.org/10.1016/j.est.2021.103439.

[89] M. Kim, S. Han, Novel Data-Efficient Mechanism-Agnostic Capacity Fade Model for Li-Ion Batteries, IEEE Trans. Ind. Electron. 68 (2021) 6267–6275. https://doi.org/10.1109/TIE.2020.2996156.

[90] E. Sarasketa-Zabala, E. Martinez-Laserna, M. Berecibar, I. Gandiaga, L.M. Rodriguez-Martinez, I. Villarreal Sarria, Realistic lifetime prediction approach for Li-ion batteries, Appl. Energy. 162 (2016) 839–852. https://doi.org/10.1016/j.apenergy.2015.10.115.

[91] R.R. Richardson, M.A. Osborne, D.A. Howey, Gaussian process regression for forecasting battery state of health, J. of Power Sources. 357 (2017) 209–219. https://doi.org/10.1016/j.jpowsour.2017.05.004.

[92] J. Lin, Y. Zhang, E. Khoo, Hybrid physics-based and data-driven modeling with calibrated uncertainty for lithium-ion battery degradation diagnosis and prognosis, Tackling Climate Change with Machine Learning: workshop at NeurIPS 2021 (2021). https://doi.org/10.48550/arXiv.2110.13661.

[93] United States Advanced Battery Consortium (USABC), Goals for Advanced Batteries for EVs. http://www.uscar.org/commands/files_download.php?files_id=364, 2019 (accessed 4.05.2021).

[94] H. Wenzl, A. Haubrock, H.-P. Beck, Degradation of Lithium Ion Batteries under Complex Conditions of Use, Zeitschrift für Physikalische Chemie. 227 (2013) 57–72. https://doi.org/10.1524/zpch.2012.0170.

[95] J.G.J. de Oliveira, V. Dhingra, C. Hametner, Feature Extraction, Ageing Modelling and Information Analysis of a Large-Scale Battery Ageing Experiment, Energies. 14 (2021). https://doi.org/10.3390/en14175295.

[96] A. Nuhic, J. Bergdolt, B. Spier, M. Buchholz, K. Dietmayer, Battery Health Monitoring and Degradation Prognosis in Fleet Management Systems, WEVJ. 9 (2018) 39. https://doi.org/10.3390/wevj9030039.

[97] F. von Bülow, F. Heinrich, T. Meisen, Fleet Management Approach for Manufacturers displayed at the Use Case of Battery Electric Vehicles, in: 2021 IEEE International Conference on Systems, Man, and Cybernetics (SMC), IEEE, 2021, pp. 3218–3225.

[98] S. Li, W. Li, C. Cook, C. Zhu, Y. Gao, Independently Recurrent Neural Network (IndRNN), in: 2018 IEEE/CVF Conference on Computer Vision and Pattern Recognition, IEEE, 2018, pp. 5457–5466.

[99] R. Pascanu, T. Mikolov, Y. Bengio, On the difficulty of training Recurrent Neural Networks, in: S. Dasgupta, D. McAllester (Eds.), Proceedings of the 30th International Conference on Machine Learning, PMLR, Atlanta, Georgia, USA, 2013, 1310-1318.

[100] A. Sass, E. Esatbeyoğlu, T. Iwwerks, Data-Driven Powertrain Component Aging Prediction Using In-Vehicle Signals, SOFSEM (Doctoral Student Research Forum) (2020). https://doi.org/.

[101] C. Zheng, W. Liu, B. Chen, D. Gao, Y. Cheng, Y. Yang, X. Zhang, S. Li, Z. Huang, J. Peng, A Data-driven Approach for Remaining Useful Life Prediction of Aircraft Engines, in: 2018 21st International Conference on Intelligent Transportation Systems (ITSC), IEEE, 2018, pp. 184–189.

[102] K.H. Hui, C.S. Ooi, M.H. Lim, M.S. Leong, S.M. Al-Obaidi, An improved wrapper-based feature selection method for machinery fault diagnosis, PloS one. 12 (2017) e0189143. https://doi.org/10.1371/journal.pone.0189143.

[103] F. Richter, O. Hartkopp, D.C. Mattfeld, Automatic Defect Detection by Classifying Aggregated Vehicular Behavior, in: M. Kryszkiewicz, A. Appice, D. Slezak, H. Rybiński, A. Skowroński, Z.W. Raś (Eds.), Foundations of intelligent systems, Springer, Cham, Switzerland, 2017, pp. 205–214.

[104] H. Liu, Y. Wang, W. Li, F. Shao, M. He, Decay mechanism and capacity prediction of lithium-ion batteries under low-temperature near-adiabatic condition, Inorg. Chem. Commun. 137 (2022). https://doi.org/10.1016/j.inoche.2021.109151.

[105] W. Li, N. Sengupta, P.A. Dechent, D.A. Howey, A. Annaswamy, D.U. Sauer, One-shot battery degradation trajectory prediction with deep learning, J. of Power Sources. 8 (2021) 230024. https://doi.org/10.1016/j.jpowsour.2021.230024.

[106] K. Liu, T.R. Ashwin, X. Hu, M. Lucu, W.D. Widanage, An evaluation study of different modelling techniques for calendar ageing prediction of lithium-ion batteries, Renewable and Sustain. Energy Rev. 131 (2020) 110017. https://doi.org/10.1016/j.rser.2020.110017.

[107] J.-z. Kong, D. Wang, T. Yan, J. Zhu, X. Zhang, Accelerated Stress Factors Based Nonlinear Wiener Process Model for Lithium-Ion Battery Prognostics, IEEE Trans. Ind. Electron. 69 (2022) 11665–11674. https://doi.org/10.1109/TIE.2021.3127035.

[108] P.K. Jones, U. Stimming, A.A. Lee, Impedance-based forecasting of lithium-ion battery performance amid uneven usage, Nature Communications. 13 (2022). https://doi.org/10.1038/s41467-022-32422-w.

[109] F. Yang, X. Song, G. Dong, K.-L. Tsui, A coulombic efficiency-based model for prognostics and health estimation of lithium-ion batteries, Energy. 171 (2019) 1173–1182. https://doi.org/10.1016/j.energy.2019.01.083.

[110] M.U. Ali, K.D. Kallu, H. Masood, K.A.K. Niazi, M.J. Alvi, U. Ghafoor, A. Zafar, Kernel recursive least square tracker and long-short term memory ensemble based battery health prognostic model, iScience. 24 (2021). https://doi.org/10.1016/j.isci.2021.103286.

[111] T. Lombardo, M. Duquesnoy, H. El-Bouysidy, F. Årén, A. Gallo-Bueno, P.B. Jørgensen, A. Bhowmik, A. Demortière, E. Ayerbe, F. Alcaide, M. Reynaud, J. Carrasco, A. Grimaud, C. Zhang, T. Vegge, P. Johansson, A.A. Franco, Artificial Intelligence Applied to Battery Research, Chemical reviews. 122 (2022) 10899–10969. https://doi.org/10.1021/acs.chemrev.1c00108.

[112] L. Yan, J. Peng, D. Gao, Y. Wu, Y. Liu, H. Li, W. Liu, Z. Huang, A hybrid method with cascaded structure for early-stage remaining useful life prediction of lithium-ion battery, Energy. 243 (2022) 123038. https://doi.org/10.1016/j.energy.2021.123038.

[113] S.J. Pan, Q. Yang, A Survey on Transfer Learning, IEEE Trans. Knowl. Data Eng. 22 (2010) 1345–1359. https://doi.org/10.1109/TKDE.2009.191.

[114] S. Shen, M. Sadoughi, M. Li, Z. Wang, C. Hu, Deep convolutional neural networks with ensemble learning and transfer learning for capacity estimation of lithium-ion batteries, Appl. Energy. 260 (2020) 114296. https://doi.org/10.1016/j.apenergy.2019.114296.

[115] L. Shao, F. Zhu, X. Li, Transfer learning for visual categorization: a survey, IEEE Trans. Neural Netw. Learn. Syst. 26 (2015) 1019–1034. https://doi.org/10.1109/TNNLS.2014.2330900.

[116] A. Warnecke, Degradation Mechanisms in NMC Based Lithium-Ion Batteries. PhD Thesis. RWTH Aachen, Aachen, Germany, 2017. http://publications.rwth-aachen.de/record/708098/files/708098.pdf.

[117] E. Braco, I. San Martin, A. Berrueta, P. Sanchis, A. Ursua, Experimental assessment of cycling ageing of lithium-ion second-life batteries from electric vehicles, J. of Energy Storage. 32 (2020). https://doi.org/10.1016/j.est.2020.101695.

[118] P.M. Attia, A. Bills, F. Brosa Planella, P. Dechent, G. dos Reis, M. Dubarry, P. Gasper, R. Gilchrist, S. Greenbank, D.A. Howey, O. Liu, E. Khoo, Y. Preger, A. Soni, S. Sripad, A.G. Stefanopoulou, V. Sulzer, Review—"Knees" in Lithium-Ion Battery Aging Trajectories, J. Electrochem. Soc. 169 (2022) 60517. https://doi.org/10.1149/1945-7111/ac6d13.

[119] S. Sun, J. Sun, Z. Wang, Z. Zhou, W. Cai, Prediction of Battery SOH by CNN-BiLSTM Network Fused with Attention Mechanism, Energies. 15 (2022) 4428. https://doi.org/10.3390/en15124428.

[120] K.L. Liu, X. Hu, Z.B. Wei, Y. Li, Y. Jiang, Modified Gaussian Process Regression Models for Cyclic Capacity Prediction of Lithium-Ion Batteries, IEEE Trans. on Transport. Electrific. 5 (2019) 1225–1236. https://doi.org/10.1109/TTE.2019.2944802.

[121] P. de Falco, L.P. Di Noia, R. RIZZO, State of Health Prediction of Lithium-Ion Batteries Using Accelerated Degradation Test Data, IEEE Trans. Ind. Appl. 57 (2021) 6483–6493. https://doi.org/10.1109/TIA.2021.3112392.

[122] D. Liu, J. Pang, J. Zhou, Y. Peng, M.G. Pecht, Prognostics for state of health estimation of lithium-ion batteries based on combination Gaussian process functional regression, Microelectronics Reliability. 53 (2013) 832–839. https://doi.org/10.1016/j.microrel.2013.03.010.

[123] J.Q. Shi, B. Wang, R. Murray-Smith, D.M. Titterington, Gaussian process functional regression modeling for batch data, Biometrics. 63 (2007) 714–723. https://doi.org/10.1111/j.1541-0420.2007.00758.x.

[124] K.-H. Pettinger, A. Kampker, C.-R. Hohenthanner, C. Deutskens, H. Heimes, A. Vom Hemdt, Lithium-ion cell and battery production processes, in: R. Korthauer (Ed.), Lithium-Ion Batteries: Basics and Applications, Springer Berlin Heidelberg, Berlin, Heidelberg, 2018, pp. 211–226.

[125] T. Baumhöfer, M. Brühl, S. Rothgang, D.U. Sauer, Production caused variation in capacity aging trend and correlation to initial cell performance, J. of Power Sources. 247 (2014) 332–338. https://doi.org/10.1016/j.jpowsour.2013.08.108.

[126] B. Bole, C.S. Kulkarni, M. Daigle, Randomized Battery Usage Data Set. https://ti.arc.nasa.gov/tech/dash/groups/pcoe/prognostic-data-repository/#batteryrnddischarge, 2012 (accessed 4.02.2021).

[127] K.A. Severson, P.M. Attia, N. Jin, N. Perkins, B. Jiang, Z. Yang, M.H. Chen, M. Aykol, P.K. Herring, D. Fraggedakis, M.Z. Bazant, S.J. Harris, W.C. Chueh, R.D. Braatz, Data-driven prediction of battery cycle life before capacity degradation, Nat. Energy. 4 (2019) 383–391. https://doi.org/10.1038/s41560-019-0356-8.

[128] B. Saha, K. Goebel, Battery Data Set. https://ti.arc.nasa.gov/tech/dash/groups/pcoe/prognostic-data-repository/#battery, 2008 (accessed 4.01.2021).

[129] D.U. Sauer, Time-series cyclic aging data on 48 commercial NMC/graphite Sanyo/Panasonic UR18650E cylindrical cells. https://doi.org/10.18154/RWTH-2021-04545, 2021 (accessed 12.07.2021).

[130] S. Grolleau, I. Baghdadi, P. Gyan, M. Ben-Marzouk, F. Duclaud, Capacity Fade of Lithium-Ion Batteries upon Mixed Calendar/Cycling Aging Protocol, WEVJ. 8 (2016) 339–349. https://doi.org/10.3390/wevj8020339.

[131] E. Figenbaum, Battery Electric Vehicle Fast Charging–Evidence from the Norwegian Market, WEVJ. 11 (2020) 38. https://doi.org/10.3390/wevj11020038.

[132] J. Neubauer, E. Wood, The impact of range anxiety and home, workplace, and public charging infrastructure on simulated battery electric vehicle lifetime utility, J. of Power Sources. 257 (2014) 12–20. https://doi.org/10.1016/j.jpowsour.2014.01.075.

[133] M.F. Jung, D. Sirkin, T.M. Gür, M. Steinert, Displayed Uncertainty Improves Driving Experience and Behavior, in: B. Begole, J. Kim, K. Inkpen, W. Woo (Eds.), CHI '15: CHI Conference on Human Factors in Computing Systems, 2015, pp. 2201–2210.

[134] Fraunhofer-Institut für System- und Innovationsforschung (ISI), Technologie-Roadmap Stationäre Energiespeicher 2030.

https://www.isi.fraunhofer.de/content/dam/isi/dokumente/cct/lib/TRM-SES.pdf, 2015 (accessed 28.11.2021).

[135] B. Tepe, J. Figgener, S. Englberger, D.U. Sauer, A. Jossen, H. Hesse, Optimal pool composition of commercial electric vehicles in V2G fleet operation of various electricity markets, Appl. Energy. 308 (2022) 118351. https://doi.org/10.1016/j.apenergy.2021.118351.

[136] M. Ghorbanzadeh, M. Astaneh, F. Golzar, Long-term degradation based analysis for lithium-ion batteries in off-grid wind-battery renewable energy systems, Energy. 166 (2019) 1194–1206. https://doi.org/10.1016/j.energy.2018.10.120.

[137] G. Pasaoglu Kilanc, D. Fiorello, A. Martino, G. Scarcella, A. Alemanno, A. Zubaryeva, C. Thiel, Driving and parking patterns of European car drivers, Publications Office of the European Union, Luxembourg, 2012.

[138] J.-F. Li, C.-H. Lin, K.-C. Chen, Cycle Life Prediction of Aged Lithium-Ion Batteries from the Fading Trajectory of a Four-Parameter Model, J. Electrochem. Soc. 165 (2018) A3634-A3641. https://doi.org/10.1149/2.0211816jes.

[139] J. Webster, R.T. Watson, Analyzing the Past to Prepare for the Future: Writing a literature Review, MIS Quarterly. 26 (2002) xiii–xxiii. https://doi.org/.

[140] Clarivate, Web of Science. https://www.webofscience.com, 2021 (accessed 13.06.2022).

[141] Universitätsbibliothek Bielefeld, Bielefeld Academic Search Engine (BASE). https://www.base-search.net, 2021 (accessed 13.06.2022).

[142] Google, Google Scholar. https://scholar.google.com, 2021 (accessed 13.06.2022).

[143] The Allen Institute for Artificial Intelligence, Semantic Scholar. https://www.semanticscholar.org, 2021 (accessed 13.06.2022).

[144] J. Vom Brocke, A. Simons, B. Niehaves, K. Riemer, R. Plattfaut, A. Cleven, Reconstructing the Giant: On the Importance of Rigour in Documenting the Literature Search Process, European Conference on Information Systems (ECIS) 2009 Proceedings (2009). https://doi.org/.

[145] B. Xu, A. Oudalov, A. Ulbig, G. Andersson, D.S. Kirschen, Modeling of Lithium-Ion Battery Degradation for Cell Life Assessment, IEEE Trans. Smart Grid. 9 (2018) 1131–1140. https://doi.org/10.1109/TSG.2016.2578950.

[146] D. Wang, J.-z. Kong, F. Yang, Y. Zhao, K.-L. Tsui, Battery prognostics at different operating conditions, Meausrement. 151 (2020) 107182. https://doi.org/10.1016/j.measurement.2019.107182.

[147] E. Redondo-Iglesias, P. Venet, S. Pelissier, Modelling Lithium-Ion Battery Ageing in Electric Vehicle Applications-Calendar and Cycling Ageing Combination Effects, Batteries-Basel. 6 (2020). https://doi.org/10.3390/batteries6010014.

[148] A.C. Cordoba-Arenas, S. Onori, Y. Guezennec, G. Rizzoni, Capacity and power fade cycle-life model for plug-in hybrid electric vehicle lithium-ion battery cells containing blended spinel and layered-oxide positive electrodes, J. of Power Sources. 278 (2015) 473–483. https://doi.org/10.1016/j.jpowsour.2014.12.047.

[149] M. Naumann, F.B. Spingler, A. Jossen, Analysis and modeling of cycle aging of a commercial LiFePO4/graphite cell, J. of Power Sources. 451 (2020). https://doi.org/10.1016/j.jpowsour.2019.227666.

[150] W. Gu, Z. Sun, X. Wei, H. Dai, A Capacity Fading Model of Lithium-Ion Battery Cycle Life Based on the Kinetics of Side Reactions for Electric Vehicle Applications, Electrochimica ACTA. 133 (2014) 107–116. https://doi.org/10.1016/j.electacta.2014.03.186.

[151] J. Olmos, I. Gandiaga, A. Saez-de-Ibarra, X. Larrea, T. Nieva, I. Aizpuru, Modelling the cycling degradation of Li-ion batteries: Chemistry influenced stress factors, J. of Energy Storage. 40 (2021). https://doi.org/10.1016/j.est.2021.102765.

[152] S. Grolleau, A. Delaille, H. Gualous, P. Gyan, R. Revel, J. Bernard, E. Redondo-Iglesias, J. Peter, S. Network, Calendar aging of commercial graphite/LiFePO4 cell - Predicting capacity fade under time dependent storage conditions, J. of Power Sources. 255 (2014) 450–458. https://doi.org/10.1016/j.jpowsour.2013.11.098.

[153] M.S. Hosen, J. Jaguemont, J. van Mierlo, M. Berecibar, Battery lifetime prediction and performance assessment of different modeling approaches, iScience. 24 (2021). https://doi.org/10.1016/j.isci.2021.102060.

[154] L. Chen, Y.Q. Tong, Z.M. Dong, Li-Ion Battery Performance Degradation Modeling for the Optimal Design and Energy Management of Electrified Propulsion Systems, Energies. 13 (2020). https://doi.org/10.3390/en13071629.

[155] A. Chu, A. Allam, A.C. Cordoba-Arenas, G. Rizzoni, S. Onori, Stochastic capacity loss and remaining useful life models for lithium-ion batteries in plug-in hybrid electric vehicles, J. of Power Sources. 478 (2020). https://doi.org/10.1016/j.jpowsour.2020.228991.

[156] J. de Hoog, J.-M. Timmermans, D. Ioan-Stroe, M.J. Swierczynski, J. Jaguemont, S. Goutam, N. Omar, J. van Mierlo, P. van den Bossche, Combined cycling and calendar capacity fade modeling of a Nickel-Manganese-Cobalt Oxide Cell with real-life profile validation, Appl. Energy. 200 (2017) 47–61. https://doi.org/10.1016/j.apenergy.2017.05.018.

[157] P. Gasper, K. Gering, E. Dufek, K. Smith, Challenging Practices of Algebraic Battery Life Models through Statistical Validation and Model Identification via Machine-Learning, J. Electrochem. Soc. 168 (2021). https://doi.org/10.1149/1945-7111/abdde1.

[158] J. Ben Ali, C. Azizi, L. Saidi, E. Bechhoefer, M. Benbouzid, Reliable state of health condition monitoring of Li-ion batteries based on incremental support vector regression with parameters optimization, Proceedings of the Institution of Mechanical Engineers, Part I: Journal of Systems and Control Engineering (2020). https://doi.org/10.1177/0959651820950849.

[159] J.M. Reniers, G. Mulder, D.A. Howey, Review and Performance Comparison of Mechanical-Chemical Degradation Models for Lithium-Ion Batteries, J. Electrochem. Soc. 166 (2019) A3189-A3200. https://doi.org/10.1149/2.0281914jes.

[160] A. Karger, L. Wildfeuer, D. Aygül, A. Maheshwari, J.P. Singer, A. Jossen, Modeling capacity fade of lithium-ion batteries during dynamic cycling considering path dependence, J. of Energy Storage. 52 (2022) 104718. https://doi.org/10.1016/j.est.2022.104718.

[161] A. Barré, F. Suard, M. Gérard, M. Montaru, D. Riu, Statistical analysis for understanding and predicting battery degradations in real-life electric vehicle use, J. of Power Sources. 245 (2014) 846–856. https://doi.org/10.1016/j.jpowsour.2013.07.052.

[162] M.S. Arulampalam, S. Maskell, N. Gordon, T.C. Clapp, A tutorial on particle filters for online nonlinear/non-Gaussian Bayesian tracking, IEEE Trans. Signal Process. 50 (2002) 174–188. https://doi.org/10.1109/78.978374.

[163] F. Cadini, C. Sbarufatti, F. Cancelliere, M. Giglio, State-of-life prognosis and diagnosis of lithium-ion batteries by data-driven particle filters, Appl. Energy. 235 (2019) 661–672. https://doi.org/10.1016/j.apenergy.2018.10.095.

[164] Y. Chang, H.J. Fang, A hybrid prognostic method for system degradation based on particle filter and relevance vector machine, Reliability Engineering and System Safety. 186 (2019) 51–63. https://doi.org/10.1016/j.ress.2019.02.011.

[165] D. Wang, J.-z. Kong, Y. Zhao, K.-L. Tsui, Piecewise model based intelligent prognostics for state of health prediction of rechargeable batteries with capacity regeneration phenomena, Meausrement. 147 (2019). https://doi.org/10.1016/j.measurement.2019.07.064.

[166] S. Kim, Y.Y. Choi, K.J. Kim, J.-I. Choi, Forecasting state-of-health of lithium-ion batteries using variational long short-term memory with transfer learning, J. of Energy Storage. 41 (2021). https://doi.org/10.1016/j.est.2021.102893.

[167] K.L. Liu, Y. Li, X. Hu, M. Lucu, W.D. Widanage, Gaussian Process Regression With Automatic Relevance Determination Kernel for Calendar Aging Prediction of Lithium-Ion Batteries, IEEE Trans. Ind. Inf. 16 (2020) 3767–3777. https://doi.org/10.1109/TII.2019.2941747.

[168] W. Li, H. Zhang, B. van Vlijmen, P. Dechent, D.U. Sauer, Forecasting battery capacity and power degradation with multi-task learning, Energy Storage Materials. 53 (2022) 453–466. https://doi.org/10.1016/j.ensm.2022.09.013.

[169] S. McLoone, G. Irwin, Improving neural network training solutions using regularisation, Neurocomputing. 37 (2001) 71–90. https://doi.org/10.1016/S0925-2312(00)00314-3.

[170] A. Aitio, D.A. Howey, Predicting battery end of life from solar off-grid system field data using machine learning, Joule. 5 (2021) 3204–3220. https://doi.org/10.1016/j.joule.2021.11.006.

[171] G. dos Reis, C. Strange, M. Yadav, S. Li, Lithium-ion battery data and where to find it, Energy and AI. 5 (2021) 100081. https://doi.org/10.1016/j.egyai.2021.100081.

[172] F. Naaz, A. Herle, J. Channegowda, A. Raj, M. Lakshminarayanan, A generative adversarial network-based synthetic data augmentation technique for battery condition evaluation, International Journal of Energy Research. 45 (2021) 19120–19135. https://doi.org/10.1002/er.7013.

[173] S. Ochella, M. Shafiee, F. Dinmohammadi, Artificial intelligence in prognostics and health management of engineering systems, Eng. Appl. of AI. 108 (2022). https://doi.org/10.1016/j.engappai.2021.104552.

[174] F. von Bülow, T. Meisen, State of Health Forecasting of Heterogeneous Lithium-ion Battery Types and Operation Enabled by Transfer Learning, PHME_CONF. 7 (2022) 490–508. https://doi.org/10.36001/phme.2022.v7i1.3312.

[175] X. Tang, K.L. Liu, X. Wang, F. Gao, J. Macro, W.D. Widanage, Model Migration Neural Network for Predicting Battery Aging Trajectories, IEEE Trans. on Transport. Electrific. 6 (2020) 363–374. https://doi.org/10.1109/TTE.2020.2979547.

[176] I. Semanjski, S. Gautama, Forecasting the State of Health of Electric Vehicle Batteries to Evaluate the Viability of Car Sharing Practices, Energies. 9 (2016) 1025. https://doi.org/10.3390/en9121025.

[177] J. Guo, Z.J. Li, M.G. Pecht, A Bayesian approach for Li-Ion battery capacity fade modeling and cycles to failure prognostics, J. of Power Sources. 281 (2015) 173–184. https://doi.org/10.1016/j.jpowsour.2015.01.164.

[178] P.M. Attia, K.A. Severson, J.D. Witmer, Statistical Learning for Accurate and Interpretable Battery Lifetime Prediction, J. Electrochem. Soc. 168 (2021) 90547. https://doi.org/10.1149/1945-7111/ac2704.

[179] R. Giorgiani do Nascimento, Lithium-ion Battery Prognosis with Variational Hybrid Physics-informed Neural Networks. PhD Thesis. University of Central Florida, Orlando, Florida, USA, 2022. https://stars.library.ucf.edu/etd2020/1011 (accessed 21.10.2022).

[180] A. Graves, Practical Variational Inference for Neural Networks, in: J. Shawe-Taylor, R. Zemel, P. Bartlett, F. Pereira, K.Q. Weinberger (Eds.), 25th Annual Conference on Neural Information Processing Systems 2011, Curran Associates, Inc., 2011.

[181] M. Lucu, E. Martinez-Laserna, I. Gandiaga, K.L. Liu, H. Camblong, W.D. Widanage, J. Marco, Data-driven nonparametric Li-ion battery ageing model aiming at learning from real operation data – Part A, J. of Energy Storage. 30 (2020) 101409. https://doi.org/10.1016/j.est.2020.101409.

[182] M. Lucu, E. Martinez-Laserna, I. Gandiaga, K.L. Liu, H. Camblong, W.D. Widanage, J. Marco, Data-driven nonparametric Li-ion battery ageing model aiming at learning from real operation data - Part B, J. of Energy Storage. 30 (2020) 101410. https://doi.org/10.1016/j.est.2020.101410.

[183] M. Lucu, M. Azkue, H. Camblong, E. Martinez-Laserna, Data-Driven Nonparametric Li-Ion Battery Ageing Model Aiming At Learning From Real Operation Data: Holistic Validation With Ev Driving Profiles, in: 2020 IEEE Energy Conversion Congress and Exposition (ECCE), 2020, pp. 5600–5607.

[184] D. Andre, C. Appel, T. Soczka-Guth, D.U. Sauer, Advanced mathematical methods of SOC and SOH estimation for lithium-ion batteries, J. of Power Sources. 224 (2013) 20–27. https://doi.org/10.1016/j.jpowsour.2012.10.001.

[185] R.R. Richardson, M.A. Osborne, D.A. Howey, Battery health prediction under generalized conditions using a Gaussian process transition model, J. of Energy Storage. 23 (2019) 320–328. https://doi.org/10.1016/j.est.2019.03.022.

[186] K.L. Liu, Q. Peng, H. Sun, M. Fei, H. Ma, T. Hu, A Transferred Recurrent Neural Network for Battery Calendar Health Prognostics of Energy-Transportation Systems, IEEE Trans. Ind. Inf. (2022) 1. https://doi.org/10.1109/TII.2022.3145573.

[187] S. Rohr, S. Müller, M. Baumann, M. Kerler, F. Ebert, D. Kaden, M. Lienkamp, Quantifying Uncertainties in Reusing Lithium-Ion Batteries from Electric Vehicles, Procedia Manufacturing. 8 (2017) 603–610. https://doi.org/10.1016/j.promfg.2017.02.077.

[188] C. Bertinelli Salucci, A. Bakdi, I.K. Glad, E. Vanem, R. de Bin, Multivariable Fractional Polynomials for lithium-ion batteries degradation models under dynamic conditions, J. of Energy Storage. 52 (2022) 104903. https://doi.org/10.1016/j.est.2022.104903.

[189] M.S. Hosen, R. Youssef, T. Kalogiannis, J. van Mierlo, M. Berecibar, Battery cycle life study through relaxation and forecasting the lifetime via machine learning, J. of Energy Storage. 40 (2021) 102726. https://doi.org/10.1016/j.est.2021.102726.

[190] S. Micari, S. Foti, A. Testa, S. de Caro, F. Sergi, L. Andaloro, D. Aloisio, G. Napoli, Reliability assessment and lifetime prediction of Li-ion batteries for electric vehicles, Electr. Eng. 104 (2022) 165–177. https://doi.org/10.1007/s00202-021-01288-4.

[191] M. Safari, M. Morcrette, A. Teyssot, C. Delacourt, Life Prediction Methods for Lithium-Ion Batteries Derived from a Fatigue Approach, J. Electrochem. Soc. 157 (2010) A892. https://doi.org/10.1149/1.3432560.

[192] E.V. Thomas, I. Bloom, J.P. Christophersen, V.S. Battaglia, Rate-based degradation modeling of lithium-ion cells, J. of Power Sources. 206 (2012) 378–382. https://doi.org/10.1016/j.jpowsour.2012.01.106.

[193] E.V. Thomas, I. Bloom, J.P. Christophersen, D.C. Robertson, L.K. Walker, C.D. Ho, V.S. Battaglia, Modeling memoryless degradation under variable stress, J. Qual. Technol. 51 (2019) 284–299. https://doi.org/10.1080/00224065.2019.1569963.

[194] S. Bamati, H. Chaoui, Lithium-Ion Batteries Long Horizon Health Prognostic Using Machine Learning, IEEE Trans. Energy Convers. 37 (2022) 1176–1186. https://doi.org/10.1109/TEC.2021.3111525.

[195] C. Birkl, D.A. Howey, Oxford Battery Degradation Dataset 1. https://doi.org/10.5287/bodleian:KO2kdmYGg, 2017 (accessed 19.10.2022).

[196] E. Chiodo, P. de Falco, L.P. Di Noia, Probabilistic Modeling of Li-Ion Battery Remaining Useful Life, IEEE Trans. on Ind. Applicat. 58 (2022) 5214–5226. https://doi.org/10.1109/TIA.2022.3170525.

[197] D. Rakhmatov, S. Vrudhula, D.A. Wallach, A model for battery lifetime analysis for organizing applications on a pocket computer, IEEE Trans. VLSI Syst. 11 (2003) 1019–1030. https://doi.org/10.1109/TVLSI.2003.819320.

[198] J.A. López-Villanueva, P.R. Iturriaga, S. Rodríguez-Bolívar, A fractional-order model for calendar aging with dynamic storage conditions, J. of Energy Storage. 50 (2022) 104537. https://doi.org/10.1016/j.est.2022.104537.

[199] J. Lu, R. Xiong, J. Tian, C. Wang, C.-W. Hsu, N.-T. Tsou, F. Sun, J. Li, Battery degradation prediction against uncertain future conditions with recurrent neural network enabled deep learning, Energy Storage Materials. 50 (2022) 139–151. https://doi.org/10.1016/j.ensm.2022.05.007.

[200] J.C. Shi, A. Rivera, D.Z. Wu, Battery health management using physics-informed machine learning, MSSP. 179 (2022). https://doi.org/10.1016/j.ymssp.2022.109347.

[201] J. Wang, Y. Xiang, Fast Modeling of the Capacity Degradation of Lithium-Ion Batteries via a Conditional Temporal Convolutional Encoder–Decoder, IEEE Trans. on Transport. Electrific. 8 (2022) 1695–1709. https://doi.org/10.1109/TTE.2021.3128018.

[202] X. Xu, S. Tang, C. Yu, J. Xie, X. Han, M. Ouyang, Remaining Useful Life Prediction of Lithium-ion Batteries Based on Wiener Process Under Time-Varying Temperature Condition, Reliability Engineering and System Safety. 214 (2021). https://doi.org/10.1016/j.ress.2021.107675.

[203] T. Endo, K. Mitsunaga, K. Takahashi, K. Kobayashi, M. Matsuishi, Damage evaluation of metals for random or varying loading—three aspects of rain flow method, Proceedings of the 1974 Symposium on Mechanical Behavior of Materials. 1 (1974) 371–380. https://doi.org/.

[204] J. Dambrowski, S. Pichlmaier, A. Jossen, Mathematical methods for classification of state-of-charge time series for cycle lifetime prediction, in: Advanced Automotive Batteries Conference Europe (AABC), 2012.

[205] A. Nuhic, R. Hu, M. Buchholz, K. Dietmayer, A health-monitoring and life-prediction approach for lithium-ion batteries based on fatigue analysis, in: Advanced Automotive Batteries Conference Europe (AABC), 2013.

[206] D.-I. Stroe, Lifetime Models for Lithium-ion Batteries used in Virtual Power Plant Applications. PhD Thesis. Aalborg University, Aalborg, Denmark, 2014. https://vbn.aau.dk/da/publications/d56e6622-f1bd-4a88-b82f-f42e6a81e86a.

[207] E. Frisk, M. Krysander, E. Larsson, Data-Driven Lead-Acid Battery Prognostics Using Random Survival Forests, Annual Conference of the PHM Society. 6 (2014). https://doi.org/10.36001/phmconf.2014.v6i1.2370.

[208] Y. Zhang, T. Wik, J. Bergström, M.G. Pecht, C. Zou, A machine learning-based framework for online prediction of battery ageing trajectory and lifetime using histogram data, J. of Power Sources. 526 (2022) 231110. https://doi.org/10.1016/j.jpowsour.2022.231110.

[209] S. Greenbank, Data-driven battery state of health diagnostics and prognostics. PhD Thesis. University of Oxford, Oxford, UK, 2022. https://ora.ox.ac.uk/objects/uuid:da0cf799-1489-4cb8-9214-4ed5be742275 (accessed 14.10.2022).

[210] P. Chanchaipo, L. Sirikul, EV battery degradation forecasting based on high dimensional data. Master Thesis. Chalmers University of Technology, Göteborg, Sweden, 2020. https://hdl.handle.net/20.500.12380/302222.

[211] R.G. Nascimento, M. Corbetta, C.S. Kulkarni, F.A.C. Viana, Hybrid physics-informed neural networks for lithium-ion battery modeling and prognosis, J. of Power Sources. 513 (2021). https://doi.org/10.1016/j.jpowsour.2021.230526.

[212] J. Hong, D. Lee, E.-R. Jeong, Y. Yi, Towards the swift prediction of the remaining useful life of lithium-ion batteries with end-to-end deep learning, Appl. Energy. 278 (2020). https://doi.org/10.1016/j.apenergy.2020.115646.

[213] F.-K. Wang, C.-Y. Huang, T. Mamo, Ensemble Model Based on Stacked Long Short-Term Memory Model for Cycle Life Prediction of Lithium–Ion Batteries, Appl. Sciences. 10 (2020) 3549. https://doi.org/10.3390/app10103549.

[214] A. Perez, F. Jaramillo, V. Quintero, M.E. Orchard, Characterizing the degradation process of Lithium-Ion Batteries using a Similarity-Based-Modeling Approach, Fourth European Conference of the Prognostics and Health Management Society 2018 (2019). https://doi.org/10.36001/phme.2018.v4i1.439.

[215] G. Ning, B. Haran, B.N. Popov, Capacity fade study of lithium-ion batteries cycled at high discharge rates, J. of Power Sources. 117 (2003) 160–169. https://doi.org/10.1016/S0378-7753(03)00029-6.

[216] P. Jones, U. Stimming, A. Lee, Impedance-based forecasting of battery performance amid uneven usage. https://doi.org/10.5281/zenodo.6645536, 2021 (accessed 20.10.2022).

[217] J. Lu, R. Xiong, J. Tian, C. Wang, C.-W. Hsu, N.-T. Tsou, F. Sun, J. Li, Battery Degradation Dataset (Fixed Current Profiles & Arbitrary Uses Profiles). https://doi.org/10.17632/kw34hhw7xg.3, 2022 (accessed 20.10.2022).

[218] W. He, N. Williard, M. Osterman, M.G. Pecht, Prognostics of lithium-ion batteries based on Dempster–Shafer theory and the Bayesian Monte Carlo method, J. of Power Sources. 196 (2011) 10314–10321. https://doi.org/10.1016/j.jpowsour.2011.08.040.

[219] S. Saxena, C. Hendricks, M.G. Pecht, Cycle life testing and modeling of graphite/LiCoO2 cells under different state of charge ranges, J. of Power Sources. 327 (2016) 394–400. https://doi.org/10.1016/j.jpowsour.2016.07.057.

[220] H.M. Barkholtz, A. Fresquez, B.R. Chalamala, S.R. Ferreira, A Database for Comparative Electrochemical Performance of Commercial 18650-Format Lithium-Ion Cells, J. Electrochem. Soc. 164 (2017) A2697-A2706. https://doi.org/10.1149/2.1701712jes.

[221] Y. Zhang, Q. Tang, Y. Zhang, J. Wang, U. Stimming, A.A. Lee, Identifying degradation patterns of lithium ion batteries from impedance spectroscopy using machine learning. https://doi.org/10.5281/zenodo.3633834, 2020 (accessed 21.10.2022).

[222] C. Shorten, T.M. Khoshgoftaar, A survey on Image Data Augmentation for Deep Learning, J. Big Data. 6 (2019) 1106. https://doi.org/10.1186/s40537-019-0197-0.

[223] X. Hu, H. Yuan, C. Zou, Z. Li, L. Zhang, Co-Estimation of State of Charge and State of Health for Lithium-Ion Batteries Based on Fractional-Order Calculus, IEEE Trans. Veh. Technol. 67 (2018) 10319–10329. https://doi.org/10.1109/TVT.2018.2865664.

[224] W. Diao, J. Jiang, C. Zhang, H. Liang, M.G. Pecht, Energy state of health estimation for battery packs based on the degradation and inconsistency, Energy Procedia. 142 (2017) 3578–3583. https://doi.org/10.1016/j.egypro.2017.12.248.

[225] M.N. Ramadan, B.A. Pramana, S.A. Widayat, L.K. Amifia, A. Cahyadi, O. Wahyunggoro, Comparative Study Between Internal Ohmic Resistance and Capacity for Battery State of Health Estimation, J. Mechatron. Electr. Power Veh. Technol. 6 (2015) 113–122. https://doi.org/10.14203/j.mev.2015.v6.113-122.

[226] J. Remmlinger, M. Buchholz, T. Soczka-Guth, K. Dietmayer, On-board state-of-health monitoring of lithium-ion batteries using linear parameter-varying models, J. of Power Sources. 239 (2013) 689–695. https://doi.org/10.1016/j.jpowsour.2012.11.102.

Author Contributions

Credit author statement:

Friedrich von Bülow: Conceptualization, Methodology, Investigation, Visualization, Writing - Original Draft, Writing - Review & Editing

Tobias Meisen: Writing - Review & Editing

Competing Interests Statement

The authors declare that they have no known competing financial interests or personal relationships that could have appeared to influence the work reported in this paper. The results, opinions and conclusions expressed in this publication are not necessarily those of Volkswagen Aktiengesellschaft.

Appendix

List of all research publications from the extend paper corpus

Table 7: List of all research publications from the extend paper corpus

Reference	Year	Type	Name
SOH forecasting models without information about future load (Section 4.1)			
[91]	2017	Journal	J. of Energy Storage
[175]	2020	Journal	IEEE Trans. on Transport. Electrific.
[177]	2015	Journal	J. of Power Sources
[176]	2016	Journal	Energies
[210]	2020	Online	Chalmers Open Digital Repository
[211]	2021	Journal	J. of Power Sources
[86]	2021	Journal	Neural Computing & Applications
[212]	2020	Journal	Appl. Energy
[127]	2019	Journal	Nat. Energy
[105]	2021	Journal	J. of Power Sources
[168]	2021	Online	Energy Storage Materials
[178]	2021	Journal	J. Electrochem. Soc.
[179]	2022	Online	PhD Thesis
SOH forecasting models without distributional information about future load (Section 4.2.1)			
[181]	2020	Journal	J. of Energy Storage
[182]	2020	Journal	J. of Energy Storage
[183]	2020	Conference	IEEE Energy Conversion Congress and Exposition (ECCE)
[153]	2021	Journal	iScience
[184]	2013	Journal	J. of Power Sources
[213]	2020	Journal	Applied Sciences
[161]	2014	Journal	J. of Power Sources
[214]	2019	Conference	European Conference of the Prognostics and Health Management Society
[120]	2019	Journal	IEEE Trans. on Transport. Electrific.
[89]	2021	Journal	IEEE Trans. Ind. Electron.
[186]	2022	Journal	IEEE Trans. Ind. Inf.

[187]	2017	Journal	Procedia Manufacturing
[188]	2021	Online	J. of Energy Storage
[189]	2021	Journal	J. of Energy Storage
[190]	2022	Journal	Electr. Eng.
[191]	2010	Journal	J. Electrochem. Soc.
[170]	2021	Journal	Joule
[192]	2012	Journal	J. of Power Sources
[193]	2019	Journal	J. of Quality Technology
[194]	2022	Journal	IEEE Trans. Energy Convers.
[196]	2022	Journal	IEEE Trans. on Ind. Applicat.
[108]	2022	Journal	Nature Communications
[198]	2022	Journal	J. of Energy Storage
[199]	2022	Journal	Energy Storage Materials
[200]	2022	Journal	Mechanical Systems and Signal Processing
[201]	2022	Journal	IEEE Trans. on Transport. Electrific.
[202]	2022	Journal	Reliability Engineering and System Safety
[107]	2022	Journal	IEEE Trans. Ind. Electron.
SOH forecasting models with information about future load based on rainflow counting (Section 4.2.2.1)			
[71]	2013	Journal	J. of Power Sources
[205]	2013	Conference	Advanced Automotive Batteries Conference Europe (AABC)
[96]	2018	Conference	Advanced Automotive Batteries Conference Europe (AABC)
[206]	2018	Journal	WEVJ
SOH forecasting models with information about future load only based on histograms (Section 4.2.2.2)			
[185]	2019	Journal	J. of Energy Storage
[88]	2021	Journal	J. of Energy Storage
[207]	2014	Conference	Annual Conference of the PHM Society
[208]	2022	Journal	J. of Power Sources
[52]	2022	Journal	IEEE Trans. Ind. Inf.
[209]	2022	Online	PhD Thesis

Capacity-based State of Health

Further Definition

Less common than the definition of SOH_{C} in Eq. (2) is the following definition [25,71]:

$$SOH_{\mathrm{C}}(t) = \frac{\mathrm{C}(t) - C_{\mathrm{EOL}}}{C_{\mathrm{nom}} - C_{\mathrm{EOL}}} \tag{14}$$

with C_{EOL} as required capacity at EOL.

Capacity-based State of Health of Series Connection

The SOH_{C} of cells in s connection is stated in Eq. (5) based on [46,48]. With the general definition of $SOH_{\mathrm{C}}(t)$ from Eq. (2) applied to cells in a series connection and the definition of C_{s} in a series connection from Eq. (3) it holds true that:

$$SOH_{\mathrm{C,s}}(t) = \frac{C_{\mathrm{s}}(t)}{C_{\mathrm{nom,s}}} = \frac{\min\limits_i C_i(t)}{\min\limits_i C_{\mathrm{nom},i}} \tag{15}$$

with $i = 1,2,\dots,n_{\mathrm{s}}$. Assuming $C_{\mathrm{nom},i} = C_{\mathrm{nom}}$, we obtain:

$$\frac{\min\limits_i C_i(t)}{\min\limits_i C_{\mathrm{nom},i}} = \frac{\min\limits_i C_i(t)}{C_{\mathrm{nom}}}. \tag{16}$$

Because of its physical meaning $C_{\mathrm{nom}} > 0$, we get:

$$\frac{\min_i C_i(t)}{C_{\text{nom}}} = \min_i \frac{C_i(t)}{C_{\text{nom}}} = \min_i SOH_{\text{C},i}(t). \tag{17}$$

Capacity-based State of Health of Parallel Connection

The SOH_{C} of cells in p connection is stated in Eq. (6) based on [46]. With the general definition of $SOH_{\text{C}}(t)$ from Eq. (2) applied to cells in a parallel connection and the definition of C_{s} in a parallel connection from Eq. (4) it holds true that:

$$SOH_{\text{C,p}}(t) = \frac{C_{\text{p}}(t)}{C_{\text{nom,p}}} = \frac{\sum_{j=1}^{n_{\text{p}}} C_j(t)}{\sum_{j=1}^{n_{\text{p}}} C_{\text{nom},j}} \tag{18}$$

with $j = 1,2,\dots,n_{\text{p}}$. Assuming $C_{\text{nom},j} = C_{\text{nom}}$, we obtain:

$$\frac{\sum_{j=1}^{n_{\text{p}}} C_j(t)}{\sum_{j=1}^{n_{\text{p}}} C_{\text{nom},j}} = \frac{\sum_{j=1}^{n_{\text{p}}} C_j(t)}{\sum_{j=1}^{n_{\text{p}}} C_{\text{nom}}} = \frac{\sum_{j=1}^{n_{\text{p}}} C_j(t)}{n_{\text{p}} \cdot C_{\text{nom}}} = \frac{1}{n_{\text{p}}} \sum_{j=1}^{n_{\text{p}}} \frac{C_j(t)}{C_{\text{nom}}} = \frac{1}{n_{\text{p}}} \sum_{j=1}^{n_{\text{p}}} SOH_{\text{C},j}(t). \tag{19}$$

Capacity-based State of Health of Parallel-Series Connections

The SOH_{C} of cells in ps connection based on [46] is stated in Eq. (7). With the general definition of $SOH_{\text{C}}(t)$ from Eq. (2) applied to cells in a ps connection and the definition of C_{p} in a parallel connection from Eq. (4) we obtain:

$$SOH_{\text{C,ps}}(t) = \frac{C_{\text{ps}}(t)}{C_{\text{nom,ps}}} = \frac{\sum_{j=1}^{n_{\text{p}}} C_{j,\text{s}}(t)}{\sum_{j=1}^{n_{\text{p}}} C_{\text{nom},j,\text{s}}} \tag{20}$$

with $j = 1,2,\dots,n_{\text{p}}$, $C_{j,\text{s}}(t)$ as capacity of the j-th series connection, and $C_{\text{nom},j,\text{s}}$ as nominal capacity of the j-th series connection. Using the definition of C_{s} in a series connection from Eq. (3), we substitute $C_{j,\text{s}}(t)$ and $C_{\text{nom},j,\text{s}}$:

$$\frac{\sum_{j=1}^{n_{\text{p}}} C_{j,\text{s}}(t)}{\sum_{j=1}^{n_{\text{p}}} C_{\text{nom},j,\text{s}}} = \frac{\sum_{j=1}^{n_{\text{p}}} \min_i C_{ji}(t)}{\sum_{j=1}^{n_{\text{p}}} \min_i C_{\text{nom},ji}} \tag{21}$$

with $i = 1,2,\dots,n_{\text{s}}$. Again assuming $C_{\text{nom},ji} = C_{\text{nom}}$ results in:

$$\frac{\sum_{j=1}^{n_{\text{p}}} \min_i C_{ji}(t)}{\sum_{j=1}^{n_{\text{p}}} \min_i C_{\text{nom},ji}} = \frac{\sum_{j=1}^{n_{\text{p}}} \min_i C_{ji}(t)}{\sum_{j=1}^{n_{\text{p}}} \min_i C_{\text{nom}}} = \frac{\sum_{j=1}^{n_{\text{p}}} \min_i C_{ji}(t)}{n_{\text{p}} \cdot C_{\text{nom}}}. \tag{22}$$

Because of its physical meaning $C_{\text{nom}} > 0$ and with Eq. (2), we get:

$$\frac{\sum_{j=1}^{n_{\text{p}}} \min_i C_{ji}(t)}{n_{\text{p}} \cdot C_{\text{nom}}} = \frac{1}{n_p} \cdot \sum_{j=1}^{n_p} \min_i \frac{C_{ji}(t)}{C_{\text{nom}}} = \frac{1}{n_{\text{p}}} \cdot \sum_{j=1}^{n_p} \min_i SOH_{\text{C},ji}(t). \tag{23}$$

Capacity-based State of Health of Series-Parallel Connections

The SOH_{C} of cells in sp connection based on [46] is stated in Eq. (8). With the general definition of $SOH_{\text{C}}(t)$ from Eq. (2) applied to cells in a sp connection and the definition of C_{s} in a series connection from Eq. (3) we obtain:

$$SOH_{\text{C,sp}}(t) = \frac{C_{\text{sp}}(t)}{C_{\text{nom,sp}}} = \frac{\min_i C_{i,\text{p}}(t)}{\min_i C_{\text{nom},i,\text{p}}} \tag{24}$$

with $i = 1,2,\dots,n_{\text{s}}$, $C_{i,\text{p}}(t)$ as capacity of the i-th parallel connection, and $C_{\text{nom},i,\text{p}}$ as nominal capacity of the i-th parallel connection. Using the definition of C_{p} in a parallel connection from Eq. (2), we substitute $C_{i,\text{p}}(t)$ and $C_{\text{nom},i,\text{p}}$:

$$\frac{\min_i C_{i,\mathrm{p}}(t)}{\min_i C_{\mathrm{nom},i,\mathrm{p}}} = \frac{\min_i \sum_{j=1}^{n_\mathrm{p}} C_{ij}(t)}{\min_i \sum_{j=1}^{n_\mathrm{p}} C_{\mathrm{nom},ij}} \tag{25}$$

with $j = 1,2,\dots,n_\mathrm{p}$. Again assuming $C_{\mathrm{nom},ij} = C_\mathrm{nom}$ results in:

$$\frac{\min_i \sum_{j=1}^{n_\mathrm{p}} C_{ij}(t)}{\min_i \sum_{j=1}^{n_\mathrm{p}} C_{\mathrm{nom},ij}} = \frac{\min_i \sum_{j=1}^{n_\mathrm{p}} C_{ij}(t)}{\min_i \sum_{j=1}^{n_\mathrm{p}} C_\mathrm{nom}} = \frac{\min_i \sum_{j=1}^{n_\mathrm{p}} C_{ij}(t)}{\min_i n_\mathrm{p} \cdot C_\mathrm{nom}} = \frac{\min_i \sum_{j=1}^{n_\mathrm{p}} C_{ij}(t)}{n_\mathrm{p} \cdot C_\mathrm{nom}}. \tag{26}$$

Because of its physical meaning $C_\mathrm{nom} > 0$ and with Eq. (2), we get:

$$\frac{\min_i \sum_{j=1}^{n_\mathrm{p}} C_{ij}(t)}{n_\mathrm{p} \cdot C_\mathrm{nom}} = \frac{1}{n_p} \cdot \sum_{j=1}^{n_p} \min_i \frac{C_{ij}(t)}{C_\mathrm{nom}} = \frac{1}{n_\mathrm{p}} \cdot \sum_{j=1}^{n_p} \min_i SOH_{\mathrm{C},ij}(t). \tag{27}$$

Relation of Capacity-based State of Health of Series-Parallel and Parallel-Series Connections

The SOH_C of cells in sp connection is greater than or equal to the SOH of cells in ps connection as stated in Eq. (9). With the definition of $SOH_{\mathrm{C,s}}$ in a series connection from Eq. (5) it holds true that:

$$SOH_{\mathrm{C,s}}(t) = \min_i SOH_{\mathrm{C},i}(t) \leq SOH_{\mathrm{C},i}(t) \tag{28}$$

with $\forall i = 1,2,\dots,n_\mathrm{s}$, e.g. the $SOH_{\mathrm{C},i}(t)$ of each cell i in a series connection is at least the minimum $SOH_{\mathrm{C,s}}(t)$ of the series connection. Considering n_p parallel connections of such a single series connection results in:

$$\sum_{j=1}^{n_\mathrm{p}} \min_i SOH_{\mathrm{C},ij}(t) \leq \sum_{j=1}^{n_\mathrm{p}} SOH_{\mathrm{C},ij}(t) \tag{29}$$

with $j = 1,2,\dots,n_\mathrm{p}$. Using the same argument as in Eq. (28) we obtain:

$$\sum_{j=1}^{n_\mathrm{p}} \min_i SOH_{\mathrm{C},ij}(t) \leq \min_i \sum_{j=1}^{n_\mathrm{p}} SOH_{\mathrm{C},ij}(t) \leq \sum_{j=1}^{n_\mathrm{p}} SOH_{\mathrm{C},ij}(t). \tag{30}$$

As by definition $n_\mathrm{p} > 0$, it follows:

$$\frac{1}{n_\mathrm{p}} \cdot \sum_{j=1}^{n_\mathrm{p}} \min_i SOH_{\mathrm{C},ij}(t) \leq \frac{1}{n_\mathrm{p}} \cdot \min_i \sum_{j=1}^{n_\mathrm{p}} SOH_{\mathrm{C},ij}(t) \tag{31}$$

which concludes our claim from Eq. (9):

$$SOH_{\mathrm{C,ps}}(t) \leq SOH_{\mathrm{C,sp}}(t). \tag{32}$$

Resistance-based State of Health

Further Definitions

Other, less common definitions compared to Eq. (1) include the relative change of the internal ohmic resistance compared to a new battery [29,223]:

$$SOH_\mathrm{R}(t) = \frac{R(t) - R_\mathrm{nom}}{R_\mathrm{nom}}. \tag{33}$$

Also, the SOH_R may refer to R_EOL as maximum R at EOL [8,35,224]:

$$SOH_\mathrm{R}(t) = \frac{R_\mathrm{EOL} - R(\mathrm{t})}{R_\mathrm{EOL} - R_\mathrm{nom}}. \tag{34}$$

As the last definition in Eq. (34), also for this definition SOH_R decreases when $R(\mathrm{t})$ increases [225,226]:

$$SOH_{\mathrm{R}}(t) = 1 + \frac{R_{\mathrm{nom}} - R(t)}{R_{\mathrm{nom}}} = 2 - \frac{R(t)}{R_{\mathrm{nom}}}. \tag{35}$$

Analogous to SOH_{C} in Eq. (2), with the last two SOH_R definitions in Eqs. (34) and (35) increasing ageing leads to a decreasing SOH.

Resistance of Series and Parallel Connections

According to Kirchhoff's junction law, the resistance of cells in series connection $R_{\mathrm{s}}(t)$ is the sum of the single cell's resistance $R_j(t)$:

$$R_{\mathrm{s}}(t) = \sum_{i=1}^{n_{\mathrm{s}}} R_i(t) \text{ with } i = 1,2,\ldots,n_{\mathrm{s}}. \tag{36}$$

The resistance of cells in parallel connection $R_{\mathrm{p}}(t)$ depends on the single cell's resistance $R_j(t)$:

$$R_{\mathrm{p}}(t) = \left(\sum_{j=1}^{n_{\mathrm{p}}} R_j(t)^{-1}\right)^{-1} \text{ with } j = 1,2,\ldots,n_{\mathrm{p}}. \tag{37}$$

Resistance-based State of Health of Series Connections

The $SOH_{\mathrm{R,s}}$ of cells in series connection depends on the cells' average $SOH_{\mathrm{R},i}(t)$ for the two applied definition of the SOH_{R}.

a) With the SOH_{R} definition from Eq. (1) $SOH_{\mathrm{R}}(t) = \frac{R(t)}{R_{\mathrm{nom}}}$ it follows for a series connection:

$$SOH_{\mathrm{R,s}}(t) = \frac{R_{\mathrm{s}}(t)}{R_{\mathrm{nom,s}}} = \frac{\sum_{i=1}^{n_{\mathrm{s}}} R_i(t)}{\sum_{i=1}^{n_{\mathrm{s}}} R_{\mathrm{nom},i}} \tag{38}$$

with $i = 1,2,\ldots,n_{\mathrm{s}}$, and Eq. (36) for the resistance of cells in series connection. Assuming $R_{\mathrm{nom},i} = R_{\mathrm{nom}}$ results in:

$$\frac{\sum_{i=1}^{n_{\mathrm{s}}} R_i(t)}{\sum_{i=1}^{n_{\mathrm{s}}} R_{\mathrm{nom},i}} = \frac{\sum_{i=1}^{n_{\mathrm{s}}} R_i(t)}{\sum_{i=1}^{n_{\mathrm{s}}} R_{\mathrm{nom}}} = \frac{\sum_{i=1}^{n_{\mathrm{s}}} R_i(t)}{n_{\mathrm{s}} \cdot R_{\mathrm{nom}}} = \frac{1}{n_{\mathrm{s}}} \cdot \sum_{i=1}^{n_{\mathrm{s}}} \frac{R_i(t)}{R_{\mathrm{nom}}}. \tag{39}$$

Finally, with the SOH_{R} definition from Eq. (1) we conclude that in series connection the $SOH_{\mathrm{R,s}}(t)$ is the cells' average $SOH_{\mathrm{R},i}(t)$:

$$\frac{1}{n_{\mathrm{s}}} \cdot \sum_{i=1}^{n_{\mathrm{s}}} \frac{R_i(t)}{R_{\mathrm{nom}}} = \frac{1}{n_{\mathrm{s}}} \cdot \sum_{i=1}^{n_{\mathrm{s}}} SOH_{\mathrm{R},i}(t). \tag{40}$$

b) With the SOH_{R} definition from Footnote 1 $SOH_{\mathrm{R}}(t) = \frac{R(t) - R_{\mathrm{nom}}}{R_{\mathrm{nom}}}$ it follows for a series connection:

$$SOH_{\mathrm{R,s}}(t) = \frac{R_{\mathrm{s}}(t) - R_{\mathrm{nom,s}}}{R_{\mathrm{nom,s}}} = \frac{\sum_{i=1}^{n_{\mathrm{s}}} R_i(t) - \sum_{i=1}^{n_{\mathrm{s}}} R_{\mathrm{nom},i}}{\sum_{i=1}^{n_{\mathrm{s}}} R_{\mathrm{nom},i}} \tag{41}$$

with $i = 1,2,\ldots,n_{\mathrm{s}}$, and Eq. (36) for the resistance of cells in series connection. Assuming $R_{\mathrm{nom},i} = R_{\mathrm{nom}}$ results in:

$$\frac{\sum_{i=1}^{n_{\mathrm{s}}} R_i(t) - \sum_{i=1}^{n_{\mathrm{s}}} R_{\mathrm{nom},i}}{\sum_{i=1}^{n_{\mathrm{s}}} R_{\mathrm{nom},i}} = \frac{\sum_{i=1}^{n_{\mathrm{s}}} (R_i(t) - R_{\mathrm{nom}})}{n_{\mathrm{s}} \cdot R_{\mathrm{nom}}} = \frac{1}{n_{\mathrm{s}}} \cdot \sum_{i=1}^{n_{\mathrm{s}}} \frac{R_i(t) - R_{\mathrm{nom}}}{R_{\mathrm{nom}}}. \tag{42}$$

Finally, with the SOH_{R} definition from Footnote 1 we conclude that in series connection the $SOH_{\mathrm{R,s}}(t)$ is the cells' average $SOH_{\mathrm{R},i}(t)$, for both SOH_{R} definitions:

$$\frac{1}{n_\mathrm{s}} \cdot \sum_{i=1}^{n_\mathrm{s}} \frac{R_i(t) - R_\mathrm{nom}}{R_\mathrm{nom}} = \frac{1}{n_\mathrm{s}} \cdot \sum_{i=1}^{n_\mathrm{s}} SOH_{\mathrm{R},i}(t). \tag{43}$$

Resistance-based State of Health of Parallel Connections

The $SOH_{\mathrm{R,p}}$ of cells in parallel connection depends on the definition of the SOH_R.

a) With the SOH_R definition from Eq. (1) $SOH_\mathrm{R}(t) = \frac{R(t)}{R_\mathrm{nom}}$ it follows for a parallel connection:

$$SOH_{\mathrm{R,p}}(t) = \frac{R_\mathrm{p}(t)}{R_{\mathrm{nom,p}}} = \frac{\left(\sum_{j=1}^{n_\mathrm{p}} R_j(t)^{-1}\right)^{-1}}{\left(\sum_{j=1}^{n_\mathrm{p}} {R_{\mathrm{nom},j}}^{-1}\right)^{-1}} = \frac{\sum_{j=1}^{n_\mathrm{p}} {R_{\mathrm{nom},j}}^{-1}}{\sum_{j=1}^{n_\mathrm{p}} R_j(t)^{-1}} \tag{44}$$

with $j = 1,2,\ldots,n_\mathrm{p}$. Assuming $R_{\mathrm{nom},j} = R_\mathrm{nom}$ results in:

$$\frac{\sum_{j=1}^{n_\mathrm{p}} {R_\mathrm{nom}}^{-1}}{\sum_{j=1}^{n_\mathrm{p}} R_j(t)^{-1}} = \frac{n_\mathrm{p}}{R_\mathrm{nom}} \cdot \frac{1}{\sum_{j=1}^{n_\mathrm{p}} R_j(t)^{-1}} = \frac{n_\mathrm{p}}{\sum_{j=1}^{n_\mathrm{p}} \frac{R_\mathrm{nom}}{R_j(t)}} = \frac{n_\mathrm{p}}{\sum_{j=1}^{n_\mathrm{p}} \left(\frac{R_j(t)}{R_\mathrm{nom}}\right)^{-1}}. \tag{45}$$

Finally, with the SOH_R definition from Eq. (1) we conclude that in parallel connection the $SOH_{\mathrm{R,p}}(t)$ is inversely dependent on the sum of the inverse s cells' $SOH_{\mathrm{R},j}(t)$:

$$\frac{n_\mathrm{p}}{\sum_{j=1}^{n_\mathrm{p}} \left(\frac{R_j(t)}{R_\mathrm{nom}}\right)^{-1}} = \frac{n_\mathrm{p}}{\sum_{j=1}^{n_\mathrm{p}} \frac{1}{SOH_{\mathrm{R},j}(t)}}. \tag{46}$$

b) With the SOH_R definition from Footnote 1 $SOH_\mathrm{R}(t) = \frac{R(t) - R_\mathrm{nom}}{R_\mathrm{nom}}$ it follows:

$$\begin{aligned} SOH_{\mathrm{R,p}}(t) &= \frac{R_\mathrm{p}(t) - R_{\mathrm{nom,p}}}{R_{\mathrm{nom,p}}} = \frac{R_\mathrm{p}(t)}{R_{\mathrm{nom,p}}} - 1 = \frac{\left(\sum_{j=1}^{n_\mathrm{p}} R_j(t)^{-1}\right)^{-1}}{\left(\sum_{j=1}^{n_\mathrm{p}} {R_{\mathrm{nom},j}}^{-1}\right)^{-1}} - 1 \\ &= \frac{\sum_{j=1}^{n_\mathrm{p}} {R_{\mathrm{nom},j}}^{-1}}{\sum_{j=1}^{n_\mathrm{p}} R_j(t)^{-1}} - 1 \end{aligned} \tag{47}$$

with $j = 1,2,\ldots,n_\mathrm{p}$. Assuming $R_{\mathrm{nom},j} = R_\mathrm{nom}$ results in:

$$\begin{aligned} \frac{\sum_{j=1}^{n_\mathrm{p}} {R_{\mathrm{nom},j}}^{-1}}{\sum_{j=1}^{n_\mathrm{p}} R_j(t)^{-1}} - 1 &= \frac{n_\mathrm{p}}{R_\mathrm{nom}} \cdot \frac{1}{\sum_{j=1}^{n_\mathrm{p}} R_j(t)^{-1}} - 1 = \frac{n_\mathrm{p}}{\sum_{j=1}^{n_\mathrm{p}} \frac{R_\mathrm{nom}}{R_j(t)}} - 1 = \frac{n_\mathrm{p}}{\sum_{j=1}^{n_\mathrm{p}} \left(\frac{R_j(t)}{R_\mathrm{nom}}\right)^{-1}} - 1 \\ &= \frac{n_\mathrm{p}}{\sum_{j=1}^{n_\mathrm{p}} \left(\frac{R_j(t)}{R_\mathrm{nom}} - 1 + 1\right)^{-1}} - 1 = \frac{n_\mathrm{p}}{\sum_{j=1}^{n_\mathrm{p}} \left(\frac{R_j(t) - R_\mathrm{nom}}{R_\mathrm{nom}} + 1\right)^{-1}} - 1. \end{aligned} \tag{48}$$

Finally, with the SOH_R definition from Footnote 1 we conclude that:

$$\frac{n_\mathrm{p}}{\sum_{j=1}^{n_\mathrm{p}} \left(\frac{R_j(t) - R_\mathrm{nom}}{R_\mathrm{nom}} + 1\right)^{-1}} - 1 = \frac{n_\mathrm{p}}{\sum_{j=1}^{n_\mathrm{p}} \frac{1}{SOH_{\mathrm{R},j}(t) + 1}} - 1. \tag{49}$$